

Review

Optical Developments in Concentrator Photovoltaic Systems—A Review

Waseem Iqbal ^{1,2} , Irfan Ullah ^{1,*}  and Seoyong Shin ^{3,*} 

¹ Department of Electrical Engineering, School of Engineering, University of Management and Technology, C-II, Johar Town, Lahore 54770, Pakistan; waseem.iqbal@umt.edu.pk

² Department of Computer Science, School of Systems and Technology, University of Management and Technology, C-II, Johar Town, Lahore 54770, Pakistan

³ Department of Information and Communication Engineering, College of ICT Convergence, Myongji University, 116 Myongji-ro, Yongin 17058, Republic of Korea

* Correspondence: irfanullah@umt.edu.pk (I.U.); sshin@mju.ac.kr (S.S.)

Abstract: Energy needs have increased with global advancements and industrial revolutions. Electrical energy utilization shares a huge amount of energy with residential and industrial loads. Traditional energy resources are expensive and polluting, producing greenhouse gasses, which is a major environmental concern. Solar energy utilization is a cost-effective, sustainable, and green solution to meet the ongoing energy demand. Concentrator photovoltaic (CPV) systems are developed for energy conversion by providing high efficiency using multi-junction solar cells. This paper provides an overview of the recent optical developments in CPV systems and emerging technologies that are likely to shape the future of CPV systems. The objective of this article is to provide an overview of the issues that need to be resolved to improve the geometrical concentration, acceptance angle, uniformity, and optical efficiency of CPV systems. A comprehensive comparison is also presented on different types of solar concentrators. In addition, future research directions are presented to facilitate the continued growth and success of CPV systems. Furthermore, this review article gives an up-to-date and widespread overview of CPV technology, assesses its potential for various applications, and distinguishes the challenges and opportunities for future research and development.

Keywords: concentrator photovoltaics (CPVs); solar concentrators; irradiance; geometrical concentration; optical efficiency; acceptance angle



Citation: Iqbal, W.; Ullah, I.; Shin, S. Optical Developments in Concentrator Photovoltaic Systems—A Review. *Sustainability* **2023**, *15*, 10554. <https://doi.org/10.3390/su151310554>

Academic Editors: Aritra Ghosh and Cristina Ventura

Received: 28 March 2023

Revised: 24 May 2023

Accepted: 22 June 2023

Published: 4 July 2023



Copyright: © 2023 by the authors. Licensee MDPI, Basel, Switzerland. This article is an open access article distributed under the terms and conditions of the Creative Commons Attribution (CC BY) license (<https://creativecommons.org/licenses/by/4.0/>).

1. Introduction

Fossil fuels, such as oil, coal, and natural gas, are widely used as a primary source of energy to fulfil the energy needs of various countries worldwide. Fossil fuels are considered as the largest source of CO₂ emissions that affect climate change, the atmosphere, temperature, and air quality, posing a serious threat to the ecosystem and environment. The fluctuating prices of primary fuels make these sources unviable energy solutions in the long run and hence lead to destabilized regions and an economic burden. To achieve the Sustainable Development Goals and reduce environmental impact, clean and green energy solutions need to be prioritized to make this planet more sustainable.

Sustainable and green energy solutions are a recent method of making this planet cleaner and safer. Electrical energy share has been gradually enlarged and currently stands at 20% [1]. RERs have attracted a market, and various RER-based models have been developed [2]. There have been varying behavioral trends and levels of social acceptance of RERs [3–5]. RERs mainly consist of solar, wind, biomass, and hydro energy, which are freely available primary sources, in contrast with traditional fossil fuels. Their different combinations have also been adopted as hybrid energy solutions [6,7]. They are free from toxic or hazardous flow gases, making them more viable and green. Wind energy has been utilized to meet energy needs, but has limitations of cut-in, rated, and furling wind speed,

which vary depending on the location [8,9]. Earth receives an amount of solar energy which is 6000 times greater than human energy needs [10]. Solar energy has dominated the energy sector as a long-lasting technology compared to other resources. A 450 GW target has been set for PVs by 2030 [1]. It is also projected that we will achieve zero CO₂ emissions by 2050 [1].

1.1. Cell Technologies for PVs and CPVs

1.1.1. Photovoltaic Cells

The conversion of sunlight into electricity is carried out using PV cells. A simple PV cell is designed using a p-n junction to harvest the sunlight (photons), and the movement of charges in a closed circuit provides the electrical energy, as shown in Figure 1 [10]. The electronic current flows from n-type contact to p-type contact, passing through the load, whereas the flow of conventional current is represented with I. Different topologies (e.g., series, parallel, and cross-tied) have been implemented to test the performance of PV technology [11]. The electrical efficiency of a PV module is based on various parameters, such as energy band gap limitations, black body radiation, solar tracking, dust, and aging factor [8,12]. A single-junction PV cell has a maximum theoretical efficiency of around 33% according to Shockley's limitations. The record efficiency of a silicon solar cell was noted as 26.7% in 2017 [13]. The efficiency of a GaAs solar cell was enhanced by up to 28.4% through an amendment of the tunneling connection and tested using the ultra-high concentration of 1500 suns [14]. Solar tracking provided an extra edge to increase the overall efficiency [15].

A PV system was tested in Ghardaia that produced 12.91% and 20.89% more energy using single- and dual-axis solar tracking, respectively [16]. In [17], a novel approach was suggested to track the sun, which achieved an energy gain in clear sky and partially cloudy environments. A mathematical model [18] of a dual-axis solar tracking system was tested for the partial CPV technology that achieved satisfactory performance in comparison with a nontracking system. In Fez, Morocco, a solar-tracking-based case study was conducted and achieved an accuracy of 0.5° using mathematical equations and Python code [19]. Furthermore, two-sided solar cells were also used to harvest the solar energy from both sides of the solar cells [20] and amorphous silicon cells were used to test the performance of the solar cells.

1.1.2. Multi-Junction (MJ) Cells

The construction of a multi-junction solar cell involves the fabrication of multiple layers of semiconductor materials with varying band gaps, stacked on top of each other to form a single device, as shown in Figure 2 [21]. The layers are arranged in such a way that the highest energy band gap material is placed at the top, while the lowest band gap material is placed at the bottom [10]. MJ junction solar cells have a higher efficiency compared to single-junction cells. In [22], a five-junction cell achieved efficiency of up to 40%. It is also noted that MJ cells achieved efficiency of 47.1% [23]. Furthermore, a triple-junction cell was used to achieve efficiency of 41% [24]. A triple-junction solar cell (10 × 10 mm²) made of GaInP/GaInAs/Ge material had electrical efficiency of 40–42% and a fill factor of 83–89% [25]. MJ solar cells have also been used in combination with solar concentrators. The solar cell material is reduced through concentration, which ultimately provides a cost-effective and efficient solution. An experiment was conducted in which a four-junction cell achieved efficiency of 46% [26]. A six-junction solar cell was evaluated and achieved efficiency of 50% [27].

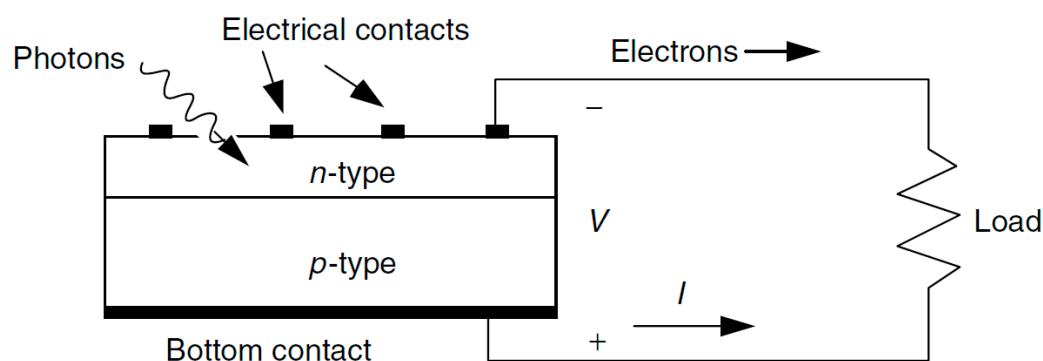


Figure 1. A generic PV cell with electron flow and conventional current (I) [10].

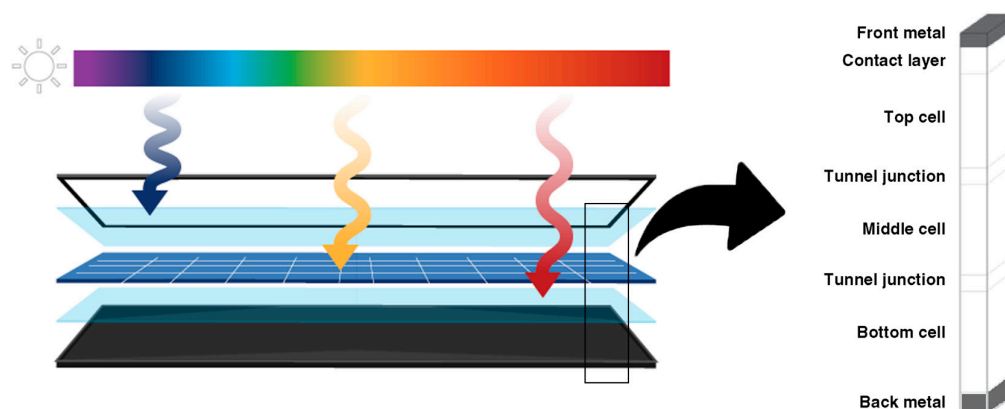


Figure 2. A multi-junction solar cell used for harvesting solar energy with different wavelengths [21]. The color bar represents different wavelengths in the solar spectrum.

1.2. Types of Solar Concentrators

In the CPV system, the light is concentrated through a solar concentrator, such as a Fresnel lens [28,29], parabolic concentrator [30], parabolic trough [31], and CPC [32]. Concentrated solar energy is divided into two categories: CPV and CSP. The heat energy produced through the concentration mechanism is used for heating purposes and electrical energy conversion. The heat energy can be used for steam generation, industrial heating processes, and space heating, making CPV/T systems highly adaptable and efficient energy solutions. Trough-based solar power plants, solar tower, and dish Stirling have been experimented on in [33]. A clear sky beam is required for the concentrator system to achieve higher efficiency. In the CSP system, a high temperature is provided to the working fluid to produce steam for further power generation process. CPV/T systems are of great interest due to their dual benefit of electricity and heating applications. In cold areas, CPV/T systems are used for domestic and commercial heating to reduce the energy cost. Furthermore, hybrid energy solutions also utilize CSP or CPV/T systems to fulfill the energy need as long-lasting and sustainable solar technologies. CPV technology has an advantage over CSP technology in terms of requiring less temperature than CSP. For solar cell energy conversion, the physical properties of the cell are used instead of transferring heat for a steam turbine.

Optical losses occurred due to misalignment between the solar cell and concentrators in both CPV and CSP systems [34–36]. The block diagram of solar concentrator systems is shown in Figure 3. In [31], a novel CPV system was developed to achieve better optical efficiency. In this study, the optical parameters that affected the efficiency of the system, such as geometrical concentration, acceptance angle, and optical efficiency, have also been discussed. A wide range of solar concentrators is presented in Figure 4 [37].

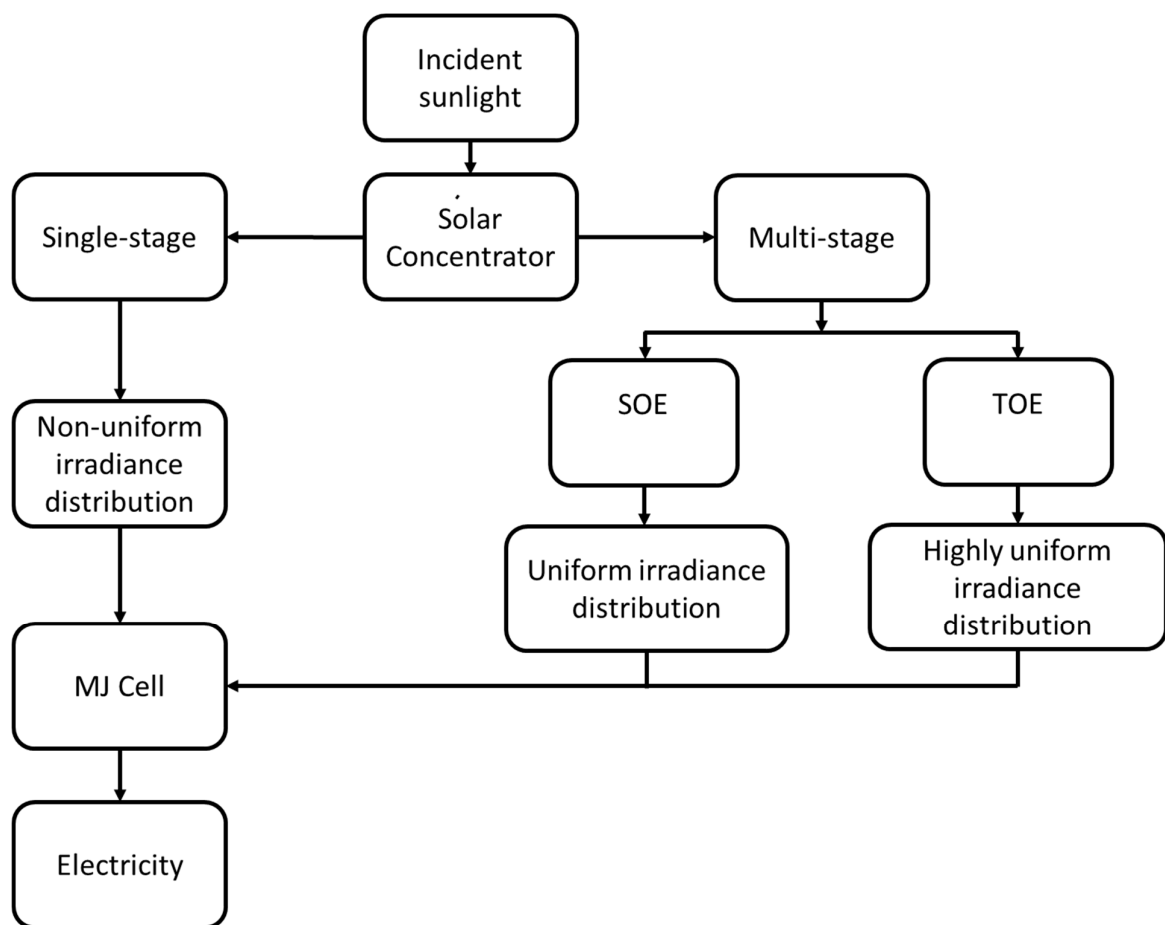


Figure 3. Block diagram of the concentrating systems.

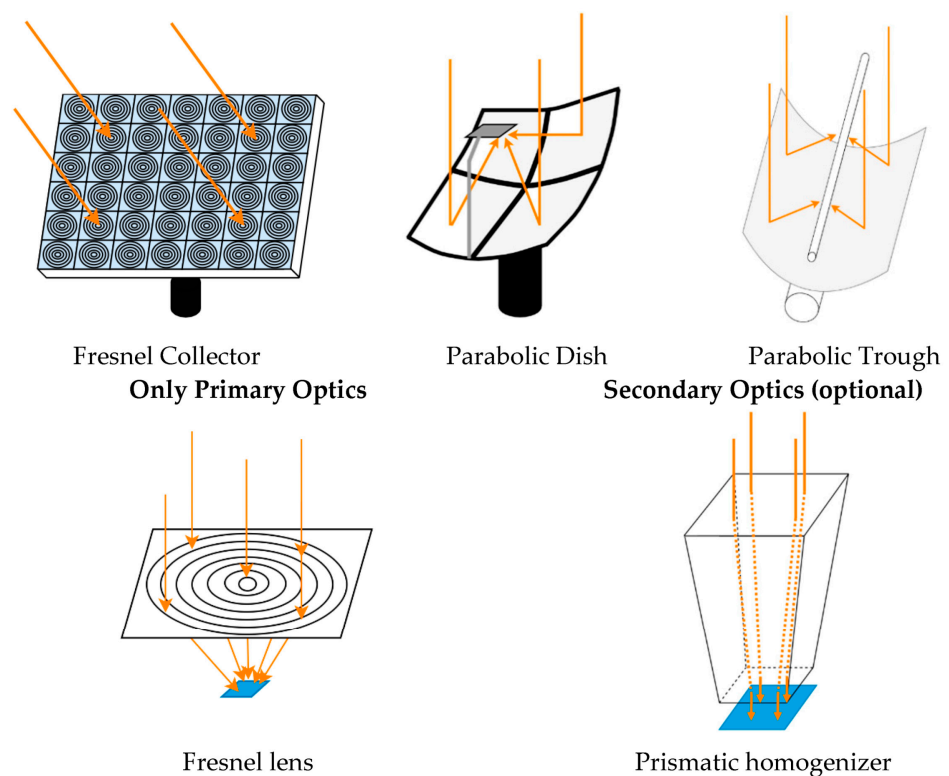


Figure 4. Different solar concentrators for CPV and CPV/T applications [37].

1.2.1. Imaging Concentrators

Spherical lenses, aspherical lenses, and reflectors are used in cameras, telescopes, microscopes, medical devices, lithography machines, etc. [38,39]. Since imaging elements make an exact focal point by which a high concentration is achieved, these optical elements (e.g., convex lens and parabolic reflector) have been used in CPV systems [30,40]. Furthermore, imaging lenses and reflectors (e.g., plano-concave lenses and convex parabolic reflectors) have also been added to CPV systems to provide uniform irradiance [41].

1.2.2. Nonimaging Concentrators

Nonimaging concentrators do not form an image of the source and have an inexact focal point, unlike imaging optics [42]. Conventional lenses and mirrors have been used in imaging devices. The CPC has been widely used as a nonimaging optical element in CPV systems [43,44]. Nonimaging optics mainly emphasize the concentration of light and irradiance distribution. Solar concentrators have been widely adopted in CPVs and CSP to reduce the area of the receiver using low-cost optical elements.

Nonuniform distribution increased the cell temperature, produced hotspots, and degraded the efficiency [45]. The issues were addressed in [41] to improve the uniformity and efficiency of the system. Furthermore, development was carried out in [30,31] by designing the concentrators using the edge-ray principle. In the simulation, the authors analyzed the optical efficiency, concentration, and irradiance uniformity.

A CPV system includes three main components: focusing optics, a tracking module, and a solar cell. A tracking device needs to be installed to receive direct sunlight for high efficiency. To design a system without tracking, the acceptance angle needs to be increased to capture the light at maximum daylight hours. The CPC, a nonimaging concentrator, is used for both CPV and CPV/T systems with and without sun-tracking [32,46]. An eight-fold Fresnel-lens-based concentrator was designed to achieve uniform irradiance [28]. A few mirror-based CPV systems were shadowed because of SOE, which was resolved using lens-based systems [31]. Fresnel-lens-based designs have been widely used in concentrator systems because of their ease of availability and fast manufacturing [47]. A nonimaging 3-D cross-compound parabolic concentrator (CCPC) was designed for the BIPV system [34]. Three rows were assembled in a parallel way; where each row consisted of three cells in the series, to test the performance. The BIPV system achieved a geometric concentration of $3.6\times$ and optical efficiency of 73.4%. Solar concentrators used in BIPV technology have added value to the energy sector. Recent findings [48] showed that the CPV system achieved a higher efficiency of 60%. It was also noticed that the area of the optical elements to be covered with the PV cells was cost-effective.

The CPV system is categorized as on-grid and off-grid, where both categories consist of a converter. A DC-DC converter is used to increase or decrease the voltage level for energy storage and utilization [49]. An inverter is also required to convert the DC to AC for the further utilization of electrical energy [50].

The CPV system has design complexity and a lack of technological standardization. The CPV/T system has achieved a low payback year of 3.45 [48]. Irrespective of the design complexity, a novel CPV system has achieved a payback time of 10–16 months [51]. Ageing and degradation over time also affect the performance of the CPV system. Ageing factors include degradation in solar concentrators (e.g., lenses, mirrors, and free-form optics). Environmental factors, such as humidity, exposure to sunlight, temperature, and climate conditions degrade the geometrical concentration and optical efficiency of the CPV system. Secondly, MJ cells also experience degradation in their performance due to the ageing factor. Direct interactions with sunlight and exposure to climate distractions degrade the performance, which results in lower electrical output power and electrical efficiency. The above-mentioned parameters also lead to a higher payback year. It was also noted that polysiloxane material was used to enhance the life of PV modules up to 50 years [20]. Furthermore, the cost of energy generation was also reduced.

2. Raytracing

To efficiently design an optical system, sequential and nonsequential raytracing are performed. In sequential raytracing, the ray path is predefined from the source to the receiver, while in nonsequential raytracing, rays travel after multiple reflections or refractions from source to target. The nonsequential raytracing of a two-stage HCPV system is illustrated in Figure 5 [52].

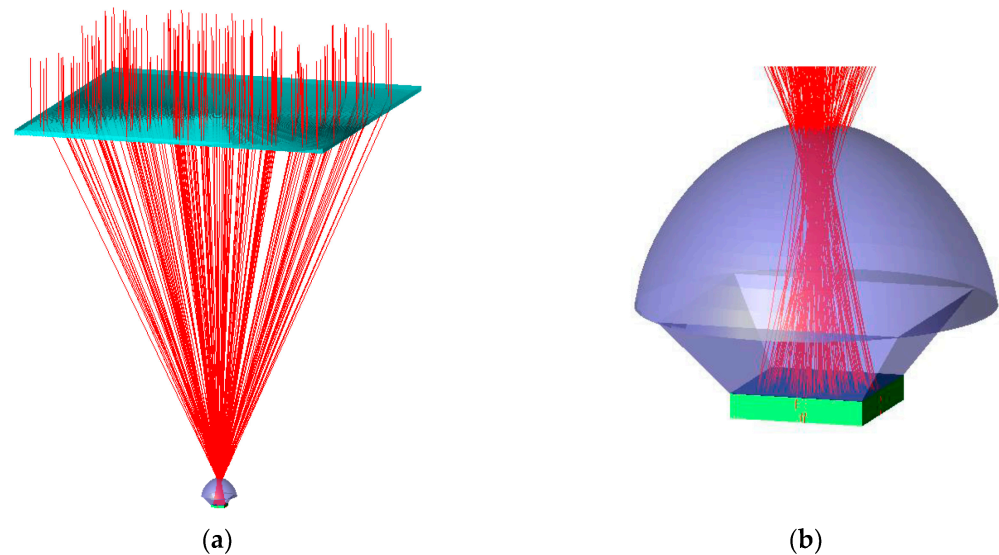


Figure 5. (a) Nonsequential raytracing diagram of an HCPV system with an acceptance angle of 1° and (b) detailed raytracing in the second stage of the system [52].

The reflected ray, irrespective of the surface's limitations, can be defined as in [42].

$$\mathbf{r}'' = \mathbf{r} - 2(\mathbf{n} \cdot \mathbf{r}) \times \mathbf{n} \quad (1)$$

The law of refraction, also known as Snell's law, deals with light rays as they pass from one medium to another, each having different refractive indices. If light travels from a high refractive index to a lower refractive index, it bends away from the normal, and on the other hand, light bends toward the normal if it travels from a low to a high refractive index medium [53]. TIR is another phenomenon which traps light within the waveguide to achieve high geometrical concentration and efficiency [54].

3. Geometrical Concentration

Geometrical concentration is the ratio of the aperture area of the concentrator over the area of the receiver, which can be calculated as in [55,56].

$$\text{Geometrical Concentration} = C_g = (\text{Aperture area of the concentrator}) / (\text{area of the receiver}) \quad (2)$$

The maximum achievable concentration (C_{\max}) has a limit for a rotational concentrator, and it is expressed by that in [57].

$$C_{\max} = 1/\sin^2(\theta) \quad (3)$$

The maximum achievable concentration for the linear concentrator is defined by that in [42].

$$C_{\max} = 1/\sin(\theta) \quad (4)$$

Nontracking CPV systems are highly dependent on the acceptance angle [58]. There is a tradeoff between the concentration and acceptance angle. Based on geometric concentration, CPV systems are classified into different categories: LCPV, MCPV, HCPV, and UHCPV [49,59]. Different solar concentrators have been developed to achieve low concentrations of $2.2\times$, $3.6\times$, $4\times$, $7\times$, and $9.93\times$ [34,60–63], medium concentrations of $23\times$, $31.31\times$, and $40\times$ [64–66], high concentrations of $128\times$, $310\times$, $610\times$, $622\times$, $707\times$, and $738\times$ [30,67–71], and ultra-high concentrations of $2300\times$, $2304\times$, $5800\times$, and $6057\times$ [72–75], respectively. Point-focused CPV systems have a high concentration, but they provide a nonuniform irradiance distribution. The system efficiency and acceptance angle decreased as the concentration increased [76]. Furthermore, SOE-based CPV systems are designed to overcome the aforementioned issue of increasing the efficiency. In [75], TOEs were used to achieve an ultra-high concentration and uniform irradiance. Moreover, cooling methods need to be installed with HCPV systems to increase the efficiency. Many cooling methods have been developed to overcome temperature issues for MJ cells [77–80]. A novel cooling method was developed using Al_2O_3 which improved the thermal and electrical efficiencies to 35.79% and 10.24%, respectively [81]. Furthermore, the output power increased to 40.86% using Al_2O_3 [82].

4. Acceptance Angle

The acceptance angle is defined as the angle at which the concentrator achieves a minimum efficiency of 90% at normal incidence [42]. The acceptance angle is one of the important parameters to be considered when designing a CPV system [83,84]. The optical performance of the CPV system is degraded as the incident angle exceeds the acceptance angle [31]. In the case of a high acceptance angle, the margin of tracking and misalignment error increases [85]; hence, the performance and efficiency of the system increase. In [58], an acceptance angle of 32° was achieved to reduce the mechanical structure and cost of the system. Moreover, a Fresnel-lens-based CPV system achieved a wider acceptance angle of 60° [64]. This novel research unlocked a path for the tracking-less CPV system. A nontracking CPV system was designed to achieve a wider acceptance angle of $\pm 44.7^\circ$ using the CPC [61]. A nontracking CPV system was developed to provide a compact and maintenance-free system in [24].

5. Irradiance Uniformity

The performance of a CPV system is dependent on irradiance uniformity, which is improved by designing various optical elements. Nonuniform irradiance distribution produces hotspots on the solar cell, which increases the temperature of the cell and hence decreases the efficiency. In [65], a linear Fresnel reflector was preferred over the parabolic trough to achieve a uniform irradiance distribution pattern, as shown in Figure 6. The feasibility report of the CPV system was presented based on the energy conversion mechanism, efficiency, and cost of the system [86]. Optical and electrical efficiencies were the essential components in calculating the performance of the system [87,88]. Optical efficiency is the ratio of light output power on the receiver to the light input power on the concentrator, which is measured according to AM 1.5: G173-03 [89],

$$\text{Optical Efficiency} = \eta_{opt} = (\text{Output light power on the receiver}) / (\text{Input light power on the concentrator}) \quad (5)$$

The electrical output power is mainly dependent on the voltage and current of the solar cell [90], where V-I characteristics are dependent upon series and parallel combinations, standard testing conditions, and direct and diffused radiations.

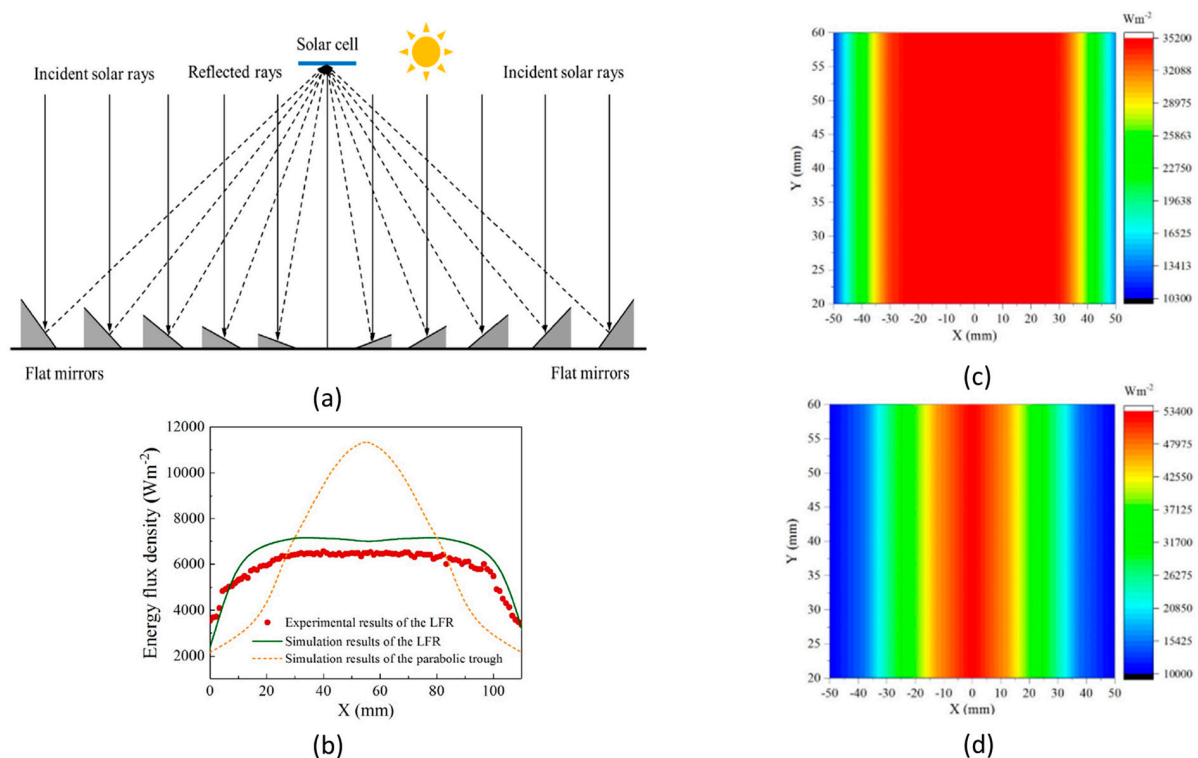


Figure 6. Comparison of the Fresnel reflector and parabolic trough: (a) schematic diagram of the linear Fresnel reflector, (b) simulation results of both systems, (c) irradiance distribution over the solar cell using linear Fresnel reflector, and (d) nonuniform irradiance distribution using parabolic trough concentrator [65].

6. Optical Developments for CPV Systems

The first solar concentrator was developed in 1976 and had a power generation capacity of one kilowatt peak [66]. Until today, various solar concentrators have been developed and modified to improve the performance of a system.

6.1. Fresnel Lens

A Fresnel lens is widely used as a POE and SOE due to its groove-based geometry, lightweight construction, and easy availability in different sizes and shapes. Fresnel-lens-based CPV systems achieved a geometrical concentration of $40\times$ using a dual-axis solar tracking system [66]. A cylindrical Fresnel lens was used in a CPV system, which achieved a geometrical concentration of $23\times$ and optical efficiency of 70%. Moreover, an acceptance angle of 60° was a striking merit of this unique design [64]. Another Fresnel-lens-based CPV system [91] was tested in Shanghai, which achieved electrical and thermal efficiencies of 16.2% and 46.6%, respectively. The HCPV system consisted of a Fresnel lens, as a primary concentrator, and the CPC as a secondary concentrator to achieve optical efficiency of 83.6% and an acceptance angle of $\pm 1.1^\circ$. Four different SOEs (trumpet, CPC, SILO-Pyramid, and refractive truncated pyramid) were tested and achieved optical efficiencies of 81%, 83.6%, 83.4%, and 81.8, respectively [92]. The hybrid Fresnel-lens-based CPV system saved $152.54 \text{ kg/m}^2/\text{year}$ CO₂ emissions [93]. In the windy areas of Japan and Korea, a 30 kilowatt Fresnel-lens-based CPV system was tested to achieve satisfactory performance [94]. In 2016, the Fresnel-lens-based two-stage concentration was preferred over single-stage concentration for better uniform irradiance [41]. In Figure 7a [68], one can see a two-stage concentrator that was designed that achieved a geometrical concentration of $310\times$ and an acceptance angle of $\pm 0.46^\circ$. The CPV system in [28] was designed using an eight-fold Fresnel-lens-based POE and SOE, as shown in Figure 7b. In the second stage of concentration, different solar concentrators, such as Fresnel RTP, XTP, SILO, FK,

and eight-fold, were used to analyze the geometrical concentration, uniform irradiance, and acceptance angle. In [95], a hybrid CPV system was designed using a Fresnel lens, pyramid, MJ solar cell, and silicon solar cell. This system achieved optical efficiencies of 94% and 85% for the direct and diffused radiations, respectively. The schematic of the HCPV system is shown in Figure 8 [95]. Table 1 presents a detailed review of various single-stage and double-stage CPV systems using the Fresnel lens, which achieved a geometrical concentration of up to $1000\times$ and optical efficiency of 88%. It also showed that a lower acceptance angle of up to $\pm 1.2^\circ$ could be achieved.

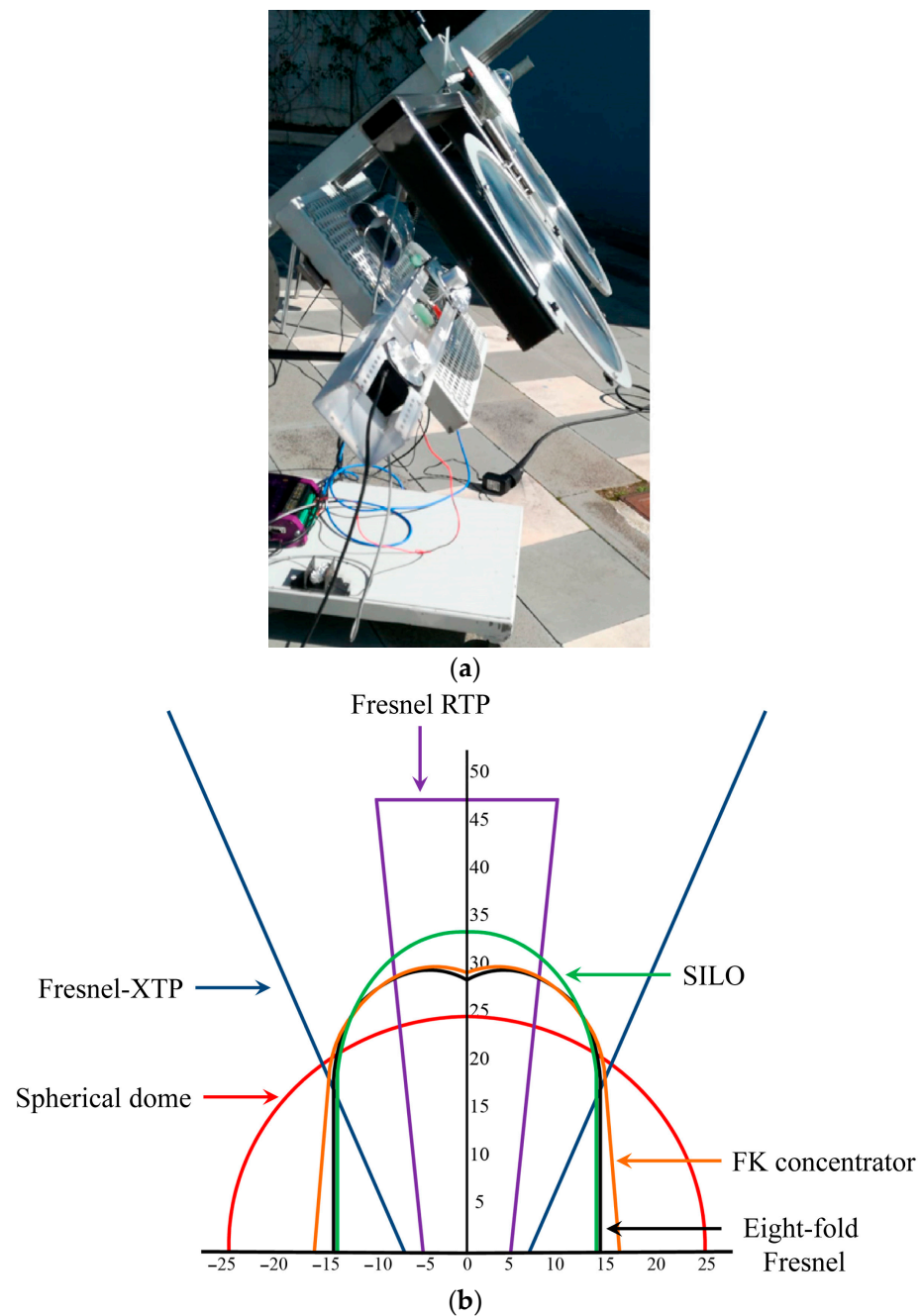


Figure 7. (a) Hardware design using a two-stage solar concentrator [68] and (b) comparison of SOEs (eight-fold, FK, RTP, SILO, spherical dome, and XTP) used for CPV systems [28].

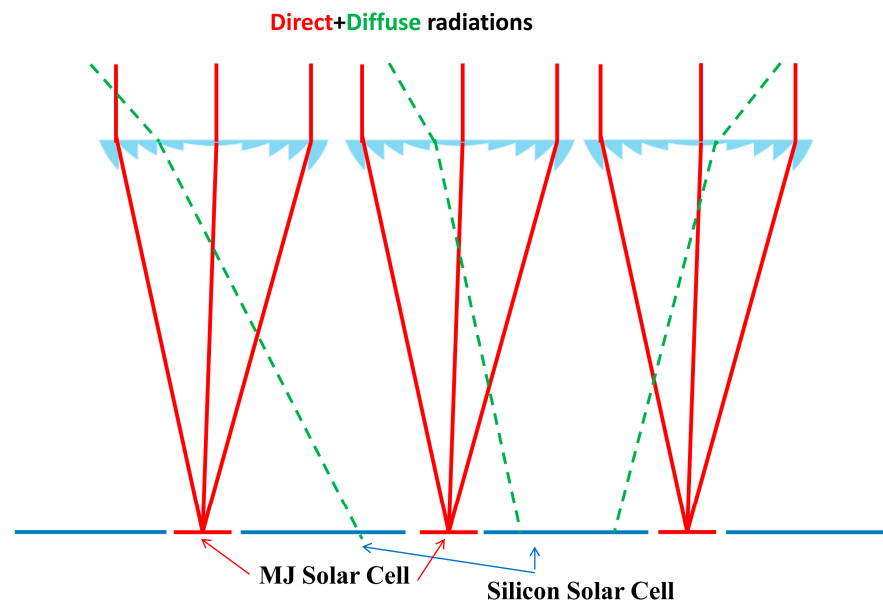


Figure 8. A schematic of hybrid CPV system, harvesting direct and diffused radiations where direct radiations are focused over the MJ solar cells using pyramid (SOE), and diffused radiations are received by Si solar cells [95].

Table 1. Comparison of single-stage and two-stage Fresnel-lens-based CPV systems representing different parameters for evaluating their performance.

Year	SOE	Technology	Cell Type	Concentration	Acceptance Angle (°)	Irradiance Uniformity	η_e (%)	η_{opt} (%)
2011 [47]	✓	CPV	MJ	-	-	-	31.5 ± 1.7	-
2012 [96]	✓	CPV	MJ	$710\times$	-	✓	32.7	-
2012 [97]	✓	CPV	MJ	$1000\times$	± 1.1	-	-	-
2013 [72]	✓	CPV	MJ	$104\times$	± 1	✓	-	82.5
2014 [28]	✓	CPV	MJ	-	-	✓	-	-
2014 [98]	✓	CPV	MJ	$1000\times$	± 1.2	-	-	83.9
2014 [99]	✓	CPV	-	$500\text{--}1000\times$	-	✓	28.6	75–82
2014 [100]	✗	CPV	Si	$210\times$	-	-	-	-
2016 [101]	✗	CPV	MJ	$260\times$	-	-	-	88
2017 [91]	-	CPV	-	-	-	-	16.2	-
2017 [92]	✓	CPV	MJ	-	± 1.03	-	-	83.6
2018 [102]	✓	CPV	MJ	$625\times$	0.73	-	30.1	-
2019 [103]	✗	CPV	MJ	$226\times$	-	✗	-	-
2020 [66]	-	CPV	Si	$40\times$	-	-	-	-
2020 [66]	-	CPV	-	$20\times$	-	-	-	-
2020 [66]	-	CPV	GaAs	$1000\times$	-	-	26	-
2020 [95]	✓	CPV	MJ	-	-	-	-	94
2021 [68]	✓	CPV	MJ	$310\times$	± 0.46	✓	-	-
2022 [64]	-	CPV	-	$23\times$	60	-	-	70
2022 [70]	-	CPV	MJ	$710\times$	0.37	-	-	24

6.2. Parabolic Trough

The parabolic trough [104] has been used in CPV and CSP systems as the primary and secondary concentrator, as shown in Figure 9 [37]. The trough provides a linear focus while a paraboloidal concentrator provides a point focus. Uniform irradiance utilizes the full area of the MJ solar cell to avoid hotspots. It is difficult to achieve uniformity in traditional single-stage parabolic concentrators. The uniform irradiance of a two-stage CPV system was achieved in [28]. A study showed that the trough-based CPV system was tested to achieve a concentration of $125\times$ and the theoretical ratio of $220\times$ [67]. The CPV/T system [105] achieved thermal and electrical efficiencies of 19.4% and 30.3%, respectively, providing high uniform irradiance. In a recent study [106], the system achieved thermal and electrical efficiencies of 46.16% and 4.83%, respectively. It was compared with the nonconcentrated system, and attained 30.3% more output. A two-stage concentrator was also used in CPV systems to achieve a geometrical concentration of $50\times$ using the trough and SOE. A line to point focus was achieved where the MJ solar cells were placed in the center to obtain an acceptance angle of $\pm 1.1^\circ$ and optical efficiency of 72% [107]. A high concentration of $600\times$ was achieved using a trough with electrical efficiency of 25% [108]. A novel CPV design [69] was simulated using the trough as the POE and micro-reflected grooves as the SOE. This CPV system achieved a geometrical concentration of $622\times$ and optical efficiency of 79%. In [109], a three-stage CPV system was designed using the parabolic trough, micro-lens, and CPC to achieve a geometric concentration of up to $1500\times$. Table 2 provides a summary of the parabolic trough concentrators used in CPV systems, and their optical parameters are also mentioned. Parabolic-trough-based CPV systems are designed to achieve a low geometrical concentration of $2.2\times$ and a high geometrical concentration of up to $1500\times$, as summarized in Table 2. Furthermore, it is shown that trough-based systems are designed to achieve electrical efficiency of up to 26.8%.



Figure 9. Parabolic trough concentrator with a focal length of 0.8 m used for CPV/T solar park located in Austria along with single-axis solar tracking system [37].

Table 2. Optical characteristics of trough-based CPV systems.

Year	SOE	Technology	Cell Type	Concentration	Acceptance Angle (°)	Irradiance Uniformity	η_e (%)	η_{opt} (%)
2013 [110]	✓	CPV		500–1500×	-	-	-	-
2014 [108]	✓	CPV	MJ	600×	-	✓	25	78
2015 [111]	✓	CPV	MJ	68×	0.6	✓	-	-
2016 [112]	✓	CPV	MJ	364×	3.2	×	20.2	-
2016 [60]	×	CPV	Si	2.2×	-	×	18.5	-
2017 [106]	-	CPV/T	-	-	-	-	4.83	-
2018 [63]	×	CPV/T	-	9.93×	-	×	-	46–62
2020 [113]	×	CPV/T	Si	20–100×	-	×	-	53
2020 [65]	×	CPV	-	31.31×	-	×	-	-
2020 [114]	✓	CPV	MJ	285×	± 1.1	✓	-	42
2021 [46]	×	CPV	MJ	107×	0.27	×	-	66.65
2021 [46]	✓	CPV	MJ	-	0.27	×	-	73
2021 [115]	×	CPV	MJ	150×	-	×	26.8	-
2021 [31]	✓	CPV	MJ	285×	± 2	✓	-	60
2022 [67]	-	CPV/T	MJ	128×	-	-	-	-
2023 [69]	✓	CPV	MJ	622×	± 0.4	✓	-	79

6.3. Compound Parabolic Concentrator (CPC)

The CPC is a nonimaging solar concentrator consisting of two parabolic curved surfaces [42]. It redirects all of the incident rays toward the receiver, as shown in Figure 10a [116]. A design using two parabolic curves, A and B, was developed to redirect the sunlight toward the flat receiver using the edge ray principle, as shown in Figure 10b [117]. An LCPV system was designed and achieved a geometrical concentration of $3.6\times$ using the CPC [34]. An integrated CPC-based CPV/T system was developed with and without glazed material, where the unglazed CPC achieved better results [118]. The CPC was also used as a secondary concentrator along with the parabolic dish concentrator to achieve optical efficiency of 68% [119]. In [107], a concentrating system using the CPC achieved a geometrical concentration of $285\times$, optical efficiency of 72%, and an acceptance angle of $\pm 1.1^\circ$. A novel CPV system for an electric vehicle was tested to be considered for different optical parameters [61]. The system achieved a geometrical concentration of $4\times$, optical efficiency of 80%, and electrical efficiency of 35%. Si-based PV cells were also used to retrieve energy from the light. A detailed comparison of CPC-based systems is presented in Table 3, which shows that a wider acceptance angle of $\pm 44.7^\circ$ was achieved in comparison with other solar concentrators. Furthermore, Table 3 depicts that the CPC has a low geometrical concentration while managing to achieve optical efficiency of 80%.

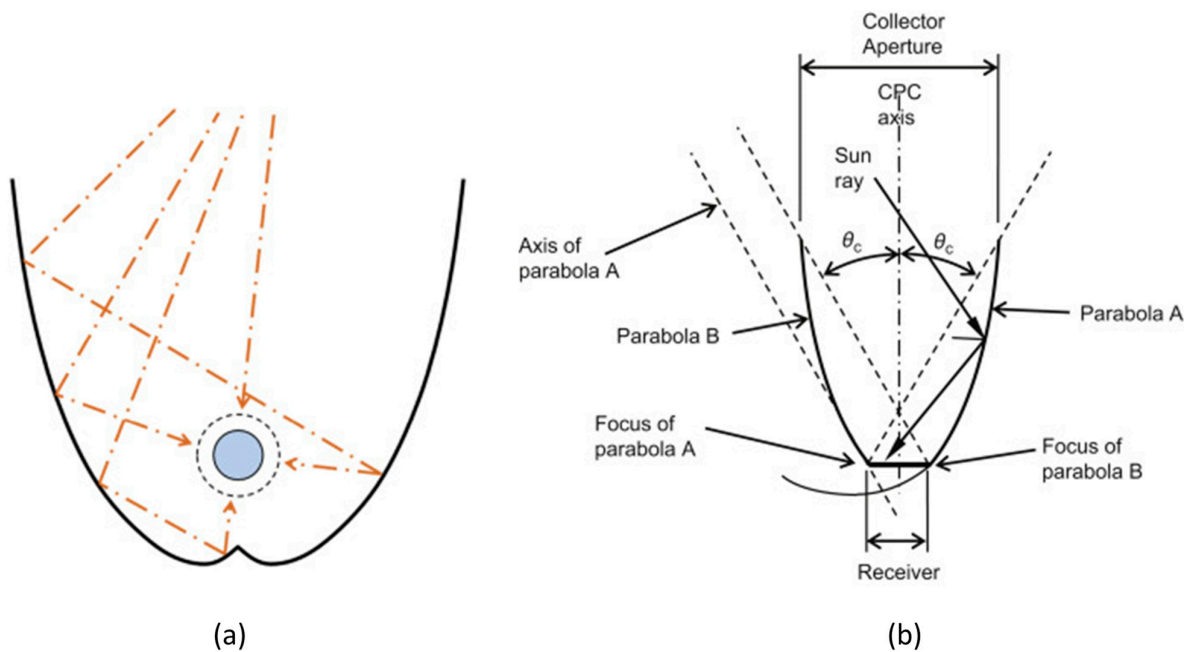


Figure 10. (a) CPC solar concentrator focusing rays on the tube receiver [116] and (b) schematic diagram of the flat receiver-based CPC [117].

Table 3. Parametric results attained using various CPC solar concentrators.

Year	POE	Technology	Cell Type	Concentration	Acceptance Angle (°)	Irradiance Uniformity	η_e (%)	η_{opt} (%)
2013 [120]	CPC	CPV/T	Si	-	± 30	×	-	80
2014 [34]	CPC	CPV	Si	$3.6\times$	-	-	-	73.4
2017 [43]	CPC	T	-	-	± 11.5	-	-	-
2021 [46]	Hybrid CPC	CPV	MJ	-	0.27	×	-	73
2022 [118]	CPC	CPV/T	Si	-	-	-	17.61	66–95
2022 [61]	CPC	CPV	MJ	$4\times$	± 44.7	-	35	78

6.4. Optical Waveguide

An optical waveguide is made of a transparent material to transmit light toward the receiver. In most CPV systems, a waveguide is used in the second stage of concentration. As shown in Figure 11, light was trapped inside the waveguide following TIR, in which the incident angle of a ray was greater than the critical angle. The system achieved a geometrical concentration of $300\times$ and optical efficiency of 81.9%. The waveguide was used to reduce the number of cells and cost of the system [121]. In the system, a primary reflector concentrated the incident light toward the waveguide, having a length of 100 mm, where the CPC increased the geometric concentration to $500\times$ [122]. In [123], a simulation of a micro-lens array with a waveguide was performed to achieve a geometrical concentration of $112.5\times$ and an acceptance angle of $\pm 1^\circ$.

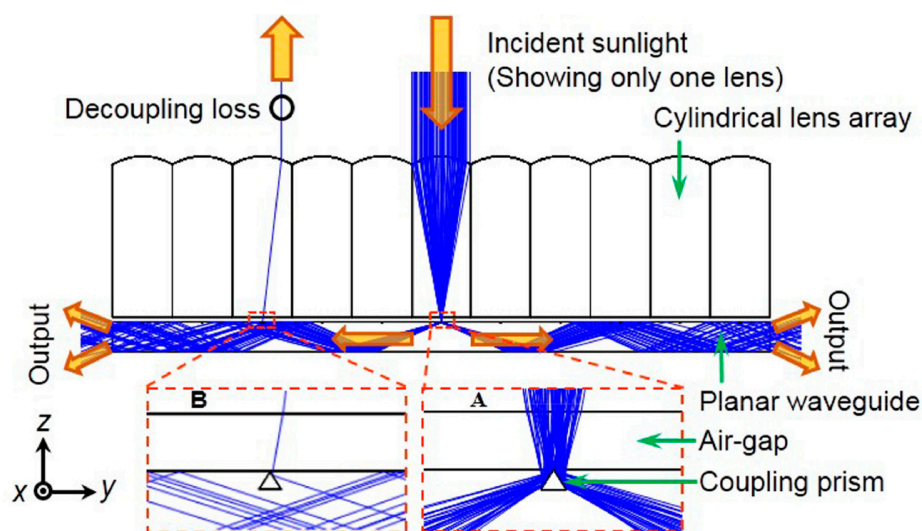


Figure 11. An optical waveguide in which TIR is used for light transmission. (A) and (B) Coupling prism is placed for redirecting the light toward the receiver to improve the efficiency of the system [54].

In Table 4, different optical-waveguide-based CPV systems have been analyzed, showing high optical efficiency of 91.5% in comparison with the Fresnel lens, parabolic trough, and CPC. Furthermore, Table 4 illustrates that an acceptance angle of $\pm 15^\circ$ was achieved using an optical waveguide. A recent study [124] was conducted to analyze different waveguide-based planar solar concentrators that consisted of luminescent solar concentrators. These concentrators performed well because of their light transmission using the TIR principle. A planar solar concentrator achieved a geometrical concentration of $738\times$ and optical efficiency of 87.5% using the POE (arc segments), light coupler, CPC, and waveguide [71]. The waveguide and the coupler were made of NBK7 glass, and the CPC was made of PMMA. Uniform irradiance was achieved in the second stage using the CPC, and an arc segment structure was used to increase the acceptance angle.

Table 4. Comparison of optical-waveguide-based CPV systems.

Year	Length	Technology	Cell Type	Concentration	Acceptance Angle ($^\circ$)	η_{opt} (%)
2010 [121]	-	CPV	MJ	$300\times$	-	81.9
2010 [123]	-	CPV	-	$112.5\times$	± 1	-
2014 [54]	-	CPV	MJ	$50\times$	± 7.5	70
2014 [122]	100 mm	CPV	-	$1200\times$	± 0.6	91.5
2014 [122]	1000 mm	CPV	-	$500\times$	± 0.6	75
2014 [122]	2000 mm	CPV	-	$1000\times$	± 0.6	52–64.5
2014 [125]	-	CPV	-	$100\times$	± 15	39
2014 [125]	-	CPV	-	$237\times$	± 9	81
2020 [71]	-	CPV	PV	$738\times$	-	87.5

6.5. Spherical Concentrators

Spherical and aspherical concentrators are used in CPV systems. In [70,126–128], spherical and aspherical lenses and reflectors were developed. Spherical lenses have issues like spherical aberration, and due to which, multiple focal points are made, while aspherical lenses and reflectors make a single focal point. A recent study [68] was conducted to compare the performance of a spherical mirror and a Fresnel lens, in which the mirror gave three times higher optical efficiency. In [129], a solar concentrator was designed

using a Fresnel lens and a modified parabolic mirror for solar laser pumping. TracePro software was used to optimize the optical components. In this novel design, the parabolic mirror was hollow in the middle, redirecting the sunlight toward the targeted surface, as shown in Figure 12. A single-stage solar concentrator achieved a flux value ranging from 4.5 to 10 MW/m² [130]. In this research, a point-focused parabolic dish concentrator was used for the hardware testing, as shown in Figure 13. Overall, both spherical and aspherical concentrators offer unique advantages in solar energy applications and can be tailored to meet specific performance requirements. An in-depth optical summary and performance evaluation of spherical and aspherical solar concentrators are presented in Table 5, which depicts higher optical efficiency of 98% in comparison with other solar concentrators. Furthermore, it shows that spherical concentrators achieved an acceptance angle of $\pm 30^\circ$ and a geometrical concentration of $1333\times$.

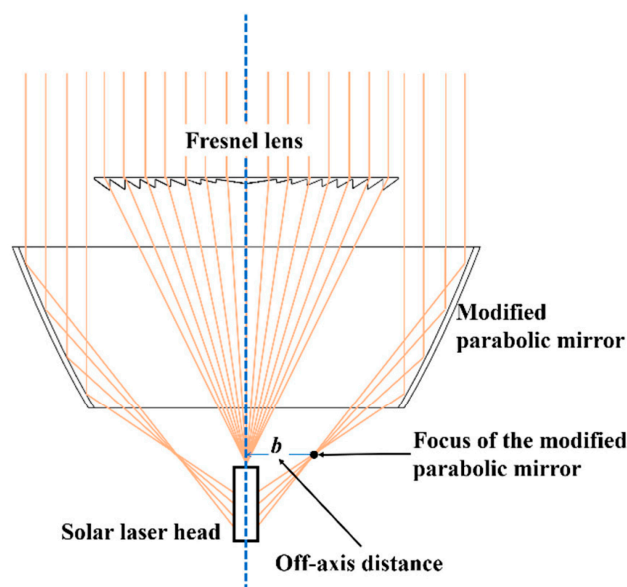


Figure 12. The lens- and mirror-based solar concentrator for solar laser pumping and nonsequential raytracing. The modified design uniformly redirects light toward the solar laser head [129].

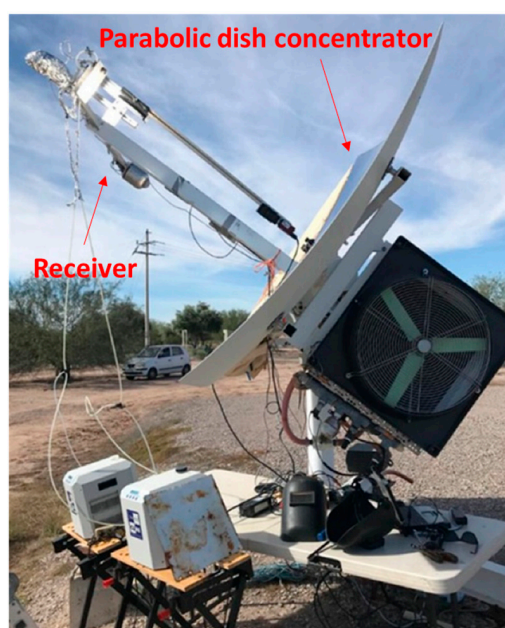


Figure 13. Hardware design using a single-stage parabolic dish concentrator [130].

Table 5. A detailed summary of spherical and aspherical solar concentrators.

Year	POE	SOE	Technology	Cell Type	Concentration	Acceptance Angle (°)	Irradiance Uniformity	η_e (%)	η_{opt} (%)
2000 [127]	Aspheric lens	✓	CPV	-	250×	± 2.6	-	-	-
2012 [62]	Parabolic mirror	✗	CPV	Si	7×	-	✗	-	-
2012 [131]	Lens	✓	CPV	MJ	380×	-	-	36.5	-
2013 [132]	Flyeye mirror	✓	CPV	MJ	1333×	± 1.3	✗	-	90
2014 [133]	Mirror	✓	CPV	MJ	500×	± 0.5	✓	28.6	-
2014 [58]	Lens array	✓	CPV	MJ	280×	± 16	-	-	-
2016 [134]	Parabolic mirror	✗	CPV/T	c-Si	20×	-	✗	10.2	-
2019 [126]	Spherical lens	✓	CPV	Si	-	-	-	-	80
2020 [119]	Parabolic dish	✓	CPV	MJ	1000×	± 30	-	-	68.3
2021 [30]	Parabolic dish	✓	CPV	MJ	610×	-	✗	-	98
2022 [128]	Parabolic mirror	✓	CPV	Si	10×	-	-	-	-
2022 [70]	Spherical mirror	-	CPV	MJ	707×	0.79	-	-	73

6.6. Micro-Level Concentrators

Micro-level CPV systems are used for small-scale applications to generate electricity. These concentrators need to be designed to overcome optical and manufacturing complexity and optical losses due to misalignment. Small-scale concentrators are designed using lenses instead of traditional metallic reflectors [125]. A light waveguide is used with the micro-concentrators by optimizing different parameters. Furthermore, geometrical concentration, total optical concentration factor, and acceptance angle are provided for rectangular and tapered systems, where the rectangular design has a geometrical concentration of $100\times$ and an acceptance angle of $\pm 15^\circ$, while the tapered design has a geometrical concentration of $237\times$ and an acceptance angle of $\pm 9^\circ$. It can be noticed that the optical concentration increases at the expense of the acceptance angle. A single-stage CPV system [135] achieves a geometrical concentration of $1000\times$ and optical efficiency of 81%. In [136], a two-stage micro-CPV system was designed using a plano-convex lens as a primary concentrator, which achieved a geometrical concentration up to $500\times$ with an acceptance angle of $\pm 1.76^\circ$. A three-stage ultra-high CPV system was designed to achieve a geometrical concentration of $938\times$, as shown in Figure 14 [75]. This ultra-high CPV system was tested for hardware and software simulations and achieved an acceptance angle of $\pm 0.30^\circ$ and $\pm 0.41^\circ$, respectively. Table 6 illustrates different CPV design configurations and optical performance parameters for small concentrators. It shows that a geometrical concentration of $<1000\times$ was achieved. Furthermore, Table 6 depicts that an acceptance angle of $\pm 15^\circ$ and optical efficiency of up to 84% were achieved.

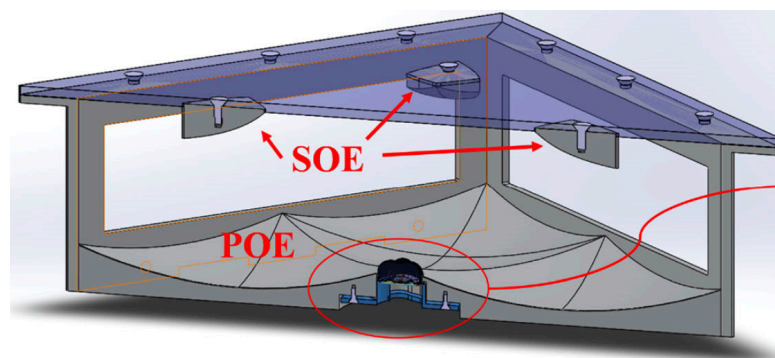
**Figure 14.** Showing a 3D design of a three-stage ultra-high CPV system [75].

Table 6. Different CPV design configurations and optical performance parameters of small concentrators.

Year	POE	SOE	Technology	Cell Type	Concentration	Acceptance Angle (°)	Irradiance Uniformity	η_e (%)	η_{opt} (%)
1995 [137]	Microgroove	×	CPV	Si	20×	-	-	21	-
2014 [125]	Micro-lens	✓	CPV	Rectangular	100×	±15	-	-	39
2014 [125]	Micro-lens	✓	CPV	Tapered	237×	±9	-	-	81
2014 [138]	Micro-lens	✓	CPV	-	100×	±2.5	-	-	84
2019 [135]	Micro-lens	×	CPV	MJ	1000×	1	×	-	81
2019 [136]	Plano-convex lens	✓	CPV	-	500×	±1.76	-	-	-
2020 [75]	Cassegrain-Koehler	✓	CPV	MJ	938×	±0.30	✓	-	31
2020 [139]	Micro-prism	✓	CPV	MJ	-	-	-	-	80

7. Discussion of Challenges and Limitations of Concentrator Photovoltaics

CPV systems have the potential to achieve higher efficiencies than traditional PV systems. There are some challenges and limitations that need to be addressed for the acceptability of CPV technology. The cost of a CPV system is generally higher than that of traditional solar panels [23,24]. The concentrators and tracking systems for concentrating sunlight over the small cells need to be cost-effective for small-scale and large-scale systems [18,19,46]. Most CPV systems require direct sunlight to operate at their maximum efficiency [95]. Thus, new optical designs should be proposed to resolve this limitation for such areas where direct sunlight is not available for a few hours of the day. CPV systems concentrate heat, which is available in the IR spectrum, which results in reducing the efficiency and lifespan if not properly cooled [77–80]. The cooling methods increased the overall cost and the complexity of CPV systems [78]. Since highly concentrated sunlight is focused on the solar cell, the surrounding area has high illumination and heat.

Table 7 presents a list of industries and institutes conducting research on improving the performance of CPV systems. The Optoelectronics Research Centre, Finland, experimented with the optical performance of multi-layer antireflective coatings used in three and five MJ solar cells to be utilized for CPV systems [140]. The Fraunhofer Institute for Solar Energy Systems ISE, Germany, manufactured triple-junction solar cells with high-power conversion efficiency of 35.9% [141]. Laboratoire Nanotechnologies Nanosystèmes (LN2)—CNRS, Canada, discusses the miniaturization of InGaP/InGaAs/Ge solar cells with optical efficiency of 33.8% for micro-CPV systems [142]. The authors from Italy experimented with the performance of a point-focused CPV system using MJ solar cells [143].

Sharp Co., Japan, announced the development of an MJ CPV module with a record-breaking conversion efficiency of 37.9% [144]. In 2023, a researcher from York University, Canada, designed a system to obtain a geometrical concentration of $7.695\times$ [145]. A recent study [146] was conducted by the National Technical University of Athens to enhance optical efficiency by 15.44%. The authors from Poland experimented with the performance of a CSP system which achieved optical efficiency of 75% and a power gain of 0.27% [147]. In [148], a CPV/T system was designed to experience an increase in the heat transfer coefficient up to 60%. The authors from Mouloud MAMMERI University of Tizi Ouzou designed a CPV system [149] that achieved a power gain of 10–13%. A Swedish company, MG Sustainable Engineering AB, experimented with a CPV/T system that achieved output power of 1140 W per collector [150].

Table 7. Recent research on CPV in various countries.

Year	Company/Institute	Country	Type	Remarks
2022 [140]	Optoelectronics Research Centre	Finland	CPV 3 MJ	Average reflectance: 5.5%
2022 [141]	Fraunhofer Institute for Solar Energy Systems ISE	Germany	CPV 3J	η_e (%): 35.9
2021 [142]	Laboratoire Nanotechnologies Nanosystèmes (LN2)—CNRS	Canada	CPV 3J	η_e (%): 33.8
2022 [143]	University of Salerno	Italy	CPV 3J	10W higher power by spherical optics
2022 [144]	Sharp	Japan	CPV 3	η_e (%): 37.9
2023 [145]	York University	Canada	CPV/T	C_g : $7.695\times$, peak flux: $30\times$
2023 [146]	National Technical University of Athens	Greece	CPV/T	Enhancement in η_{opt} (%): 15.44
2023 [147]	Silesian University of Technology	Poland	CSP	η_{opt} (%): 75, power gain: 0.27%
2023 [148]	Universitat Politècnica de Catalunya (UPC)	Spain	CPV/T	Increase in heat transfer coefficient: 60%
2023 [149]	Mouloud MAMMERI University of Tizi Ouzou	Algeria	CPV	Power gain: 10–13%, η_{opt} (%) of receiver: 100
2023 [150]	MG Sustainable Engineering AB	Sweden	CPV/T	Output power per collector: 1140 W

8. Conclusions and Future Recommendations

Researchers have developed various CPV systems to improve optical efficiency by increasing concentration, irradiance uniformity, and acceptance angle. In this article, various CPV systems were studied and compared to find out deficiencies and provide recommendations for the improvement. This review study mainly focused on recent developments in concentrator technology. Improving the efficiency of solar cells is a critical step in enhancing the overall performance of the CPV system. This can be achieved by using higher-quality materials, optimizing the cell design, or incorporating novel manufacturing techniques. Manufacturing advancement in MJ solar cells made it possible to add more layers to increase the efficiency—four-junction and six-junction solar cells achieved optical efficiencies of 46% and 50%, respectively. One of the issues in MJ solar cells is the nonuniformity, which has been resolved by researchers using nonimaging optical concentrators.

The design of the concentrator can have a significant impact on the system's performance. Various parameters, such as the concentrator's shape, size, and materials, can be optimized to achieve better concentration levels and reduce losses due to reflection or scattering. Most systems use the parabolic reflector and Fresnel lens as the main concentrators because of their advantages over the other concentrators. The parabolic trough concentrator is the most promising solar concentrator, which has been widely used in CPV and CSP systems. The trough is a reflector that has higher optical efficiency and minimum losses in comparison with the Fresnel lens. Most of the single-stage systems had nonuniformity issues that were resolved by introducing multiple optical elements. A high concentration should be achieved to increase the output power of the solar cell. Since a high concentration increases the cell temperature, efficient cooling methods should be developed. Different wavelengths in the solar spectrum should be mixed up to distribute the uniform spectrum over the solar cell to increase the efficiency of the system.

Researchers have developed nontracking CPV systems to reduce mechanical hardware components. Since the roof-top of a building has limited space, CPV systems should be developed for the envelope of multi-floor buildings. Similarly, for vehicle-based CPV systems, nontracking small concentrators with a high acceptance angle should be developed.

The optical parameters of various CPV systems were compared. It was found that few systems achieved an acceptance angle of $<2^\circ$, while nontracking systems achieved an acceptance angle of $<60^\circ$. Advanced tracking systems can help to maintain the alignment

between the concentrator and the sun, improving the system's overall performance. The acceptance angle increases at the cost of efficiency. Most of the single-stage trough and linear Fresnel-lens-based systems achieved a concentration of $<50\times$. However, other concentrators, such as the paraboloidal reflector, Fresnel lens, and CPC, gave a higher concentration of up to $1500\times$. To further increase the concentration, novel designs of concentrating modules should be designed using widely used concentrators, which will eventually increase the performance of CPV systems. In most of the concentrators, hardware and manufacturing complexity was noticed. Different CPV designs are under development to overcome the aforesaid issues. At present, CPV systems achieve maximum optical efficiency of 70%.

For the potential commercialization of CPV systems, devices should be compact, simple in design, and cost-effective. Despite their great promise, CPV systems suffer from different issues: cleaning, aging degradation, deficiency of technology standardization, and social acceptance. The performance of a CPV system can be affected by environmental factors, such as temperature, humidity, and dust. By considering these factors during the system design and operation, it is possible to improve the system's overall performance and reliability. Cost-effective MJ cells should be developed to be used in CPV technology for enhancing efficiency. Additionally, novel optical elements need to be developed to be integrated with MJ cells.

Future developments should aim to expand the applicability of CPV systems to a wider range of geographical locations, including regions with a lower DNI. This can be achieved through advancements in concentrator optics, tracking systems, and system integration with other renewable energy technologies, such as energy storage and hybrid systems. Future research should concentrate on enhancing CPV systems' dependability and toughness through the use of premium components, sturdy construction, and efficient thermal management strategies.

Author Contributions: Conceptualization, W.I.; writing—original draft preparation, W.I.; writing—review and editing, I.U.; supervision, I.U. and S.S.; funding acquisition, S.S. All authors have read and agreed to the published version of the manuscript.

Funding: This work was supported under the framework of the international cooperation program managed by the National Research Foundation of Korea (project number NRF-2022K2A9A1A06092471) and NRF grant funded by the Korean government (MIST) (project number 2021R1A2C1010879).

Data Availability Statement: Not applicable.

Conflicts of Interest: The authors declare no conflict of interest.

Nomenclature

PV	Photovoltaic
RER	Renewable energy resource
CPV	Concentrator photovoltaic
LCPV	Low concentrator photovoltaic
MCPV	Medium concentrator photovoltaic
HCPV	High concentrator photovoltaic
UHCPV	Ultra-high concentrator photovoltaic
CPV/T	Concentrator photovoltaic thermal
BIPV	Building-integrated photovoltaic
CSP	Concentrator solar power
CPC	Compound parabolic concentrator
SILO	Single-lens optical element
FK	Fresnel–Köhler
RTP	Refractive truncated pyramid
MJ	Multi-junction
C_{\max}	Maximum achievable concentration
θ	Acceptance angle

C_g	Geometrical concentration ratio
TIR	Total internal reflection
POE	Primary optical element
SOE	Secondary optical element
TOE	Tertiary optical element
η_{opt}	Optical efficiency
PMMA	Polymethyl methacrylate
η_e	Electrical efficiency
r	Unit vectors along incident rays
r''	Unit vectors along reflected rays
n	Unit vector along the normal pointing into the reflecting surface

References

1. International Energy Agency (IEA). 2021. Available online: <https://www.iea.org/reports/world-energy-outlook-2021> (accessed on 31 August 2022).
2. Akarsua, B.; Genc, M.S. Optimization of electricity and hydrogen production with hybrid renewable energy systems. *Fuel* **2022**, *334*, 124465. [\[CrossRef\]](#)
3. Park, E. Social Acceptance of Renewable Energy Technologies in the Post-fukushima Era. *Front. Psychol.* **2021**, *11*, 612090. [\[CrossRef\]](#) [\[PubMed\]](#)
4. Masrahi, A.; Wang, J.-H.; Abudiyah, A.K. Factors influencing consumers' behavioral intentions to use renewable energy in the United States residential sector. *Energy Rep.* **2021**, *7*, 7333–7344. [\[CrossRef\]](#)
5. Lerman, L.V.; Benitez, G.B.; Gerstlberger, W.; Rodrigues, V.P.; Frank, A.G. Sustainable conditions for the development of renewable energy systems: A triple bottom line perspective. *Sustain. Cities Soc.* **2021**, *75*, 103362. [\[CrossRef\]](#)
6. Ikelle, L.T. Chapter 16: Biomass, Solar, and Wind Energy Resources: Fundamentals and Technology. In *Introduction to Earth Sciences*, 2nd ed.; World Scientific Publishing Co.: Singapore, 2020; pp. 683–734.
7. Ahmad, J.; Imran, M.; Khalid, A.; Iqbal, W.; Ashraf, S.R.; Adnan, M.; Ali, S.F.; Khokhar, K.S. Techno economic analysis of a wind-photovoltaic-biomass hybrid renewable energy system for rural electrification: A case study of Kallar Kahar. *Energy* **2018**, *148*, 208–234. [\[CrossRef\]](#)
8. Cheng, C.; Blakers, A.; Stocks, M.; Lu, B. 100% renewable energy in Japan. *Energy Convers. Manag.* **2022**, *255*, 115299. [\[CrossRef\]](#)
9. Al-Ghussain, L.; Ahmad, A.D.; Abubaker, A.M.; Hassan, M.A. Exploring the feasibility of green hydrogen production using excess energy from a country-scale 100% solar-wind renewable energy system. *Int. J. Hydrogen Energy* **2022**, *47*, 21613–21633. [\[CrossRef\]](#)
10. Masters, G.M. Photovoltaic Materials and Electrical Characteristics. In *Renewable and Efficient Electric Power Systems*; John Wiley & Sons, Inc.: Hoboken, NJ, USA, 2004; pp. 445–504.
11. Chadge, R.B.; Sunheriya, N.; Giri, J.P.; Shrivastava, N. Experimental investigation of different electrical configurations and topologies for Photovoltaic system. *Mater. Today Proc.* **2022**, *57*, 316–320. [\[CrossRef\]](#)
12. Gholami, A.; Ameri, M.; Zandi, M.; Ghoachani, R.G. Electrical, thermal and optical modeling of photovoltaic systems: Step-by-step guide and comparative review study. *Sustain. Energy Technol. Assess.* **2022**, *49*, 101711. [\[CrossRef\]](#)
13. Andreani, L.C.; Bozzola, A.; Kowalczewski, P.; Liscidini, M.; Redorici, L. Silicon solar cells: Toward the efficiency limits. *Adv. Physics X* **2019**, *4*, 1548305. [\[CrossRef\]](#)
14. Yamaguchi, M.; Luque, A. High efficiency and high concentration in photovoltaics. *IEEE Trans. Electron Devices* **1999**, *46*, 2139–2144. [\[CrossRef\]](#)
15. Ramaneti, K.; Kakani, P.; Prakash, S. Improving Solar Panel Efficiency by Solar Tracking and Tilt Angle Optimization with Deep Learning. In Proceedings of the 5th International Conference on Smart Grid and Smart Cities (ICSGSC), Tokyo, Japan, 18–20 June 2021.
16. Zaghba, L.; Khennane, M.; Mekhilef, S.; Fezzani, A.; Borni, A. Experimental outdoor performance assessment and energy efficiency of 11.28 kWp grid tied PV systems with sun tracker installed in saharan climate: A case study in Ghardaia, Algeria. *Sol. Energy* **2022**, *243*, 174–192. [\[CrossRef\]](#)
17. Achkari, O.; El Fadar, A.; Amlal, I.; Haddi, A.; Hamidoun, M.; Hamdoune, S. A new sun-tracking approach for energy saving. *Renew. Energy* **2021**, *169*, 820–835. [\[CrossRef\]](#)
18. Sato, D.; Yamagata, Y.; Hirata, K.; Yamada, N. Mathematical power-generation model of a four-terminal partial concentrator photovoltaic module for optimal sun-tracking strategy. *Energy* **2020**, *213*, 118854. [\[CrossRef\]](#)
19. Ourraoui, I.; Ahaitouf, A. Investigation of the feasibility and potential use of sun tracking solutions for concentrated photovoltaic Case study Fez Morocco. *Energy Rep.* **2022**, *8*, 1412–1425. [\[CrossRef\]](#)
20. Panchenko, V.; Izmailov, A.; Kharchenko, V.; Lobachevskiy, Y. Photovoltaic Solar Modules of Different Types and Designs for Energy Supply. *Int. J. Energy Optim. Eng.* **2020**, *9*, 74–94. [\[CrossRef\]](#)
21. Multi-Junction Solar Cells: What You Need to Know. Available online: <https://news.energysage.com/multijunction-solar-cells/> (accessed on 4 March 2023).

22. Green, M.A.; Dunlop, E.D.; Hohl-Ebinger, J.; Yoshita, M.; Kopidakis, N.; Bothe, K.; Hinken, D.; Rauer, M.; Hao, X. Solar Cell Efficiency Tables (Version 60). *Prog. Photovolt. Res. Appl.* **2022**, *30*, 687–701. [\[CrossRef\]](#)
23. Baiju, A.; Yarema, M. Status and challenges of multi-junction solar cell technology. *Front. Energy Res.* **2022**, *10*, 971918. [\[CrossRef\]](#)
24. Kitai, A. Tracking-free adaptive contact concentration photovoltaics. *OSA Contin.* **2020**, *3*, 163. [\[CrossRef\]](#)
25. Azure Space Solar Power GmbH. 2015. Available online: http://www.azurspace.com/images/products/0004355-00-01_3C44_AzurDesign_10x10.pdf (accessed on 1 September 2022).
26. Dimroth, F.; Tibbits, T.N.; Niemeyer, M.; Predan, F.; Beutel, P.; Karcher, C.; Oliva, E.; Siefer, G.; David, L.; Fuß-Kailuweit, P. Four-Junction Wafer-Bonded Concentrator. *IEEE J. Photovolt.* **2016**, *6*, 343–349. [\[CrossRef\]](#)
27. Geisz, J.F.; Steiner, M.A.; Jain, N.; Schulte, K.L.; France, R.M.; McMahon, W.E.; Perl, E.E.; Friedman, D.J. Building a Six-Junction Inverted Metamorphic Concentrator Solar Cell. *IEEE J. Photovolt.* **2018**, *8*, 626–632. [\[CrossRef\]](#)
28. Ullah, I. Development of Fresnel-based Concentrated Photovoltaic (CPV) System with Uniform Irradiance. *J. Daylighting* **2014**, *1*, 2–7. [\[CrossRef\]](#)
29. Sharma, P.; Walker, A.W.; Wheeldon, J.F.; Hinzer, K.; Schriemer, H. Enhanced Efficiencies for High-Concentration, Multijunction PV Systems by Optimizing Grid Spacing under Nonuniform Illumination. *Int. J. Photoenergy* **2014**, *2014*, 582083. [\[CrossRef\]](#)
30. Oh, S.J.; Kim, H.; Hong, Y. Monte Carlo Ray-Tracing Simulation of a Cassegrain Solar Concentrator Module for CPV. *Front. Energy Res.* **2021**, *9*, 722842. [\[CrossRef\]](#)
31. Ullah, I. Optical design of centered-receiver trough-based CPV system. *J. Photon. Energy* **2021**, *11*, 035502. [\[CrossRef\]](#)
32. Jiang, C.; Yu, L.; Yang, S.; Li, K.; Wang, J.; Lund, P.D.; Zhang, Y. A Review of the Compound Parabolic Concentrator (CPC) with a Tubular Absorber. *Energies* **2020**, *13*, 695. [\[CrossRef\]](#)
33. Pitz-Paal, R. Concentrating Solar Power. In *Future Energy Improved, Sustainable and Clean Options for Our Planet*, 3rd ed.; Elsevier: Amsterdam, The Netherlands, 2020; pp. 413–430.
34. Baig, H.; Sellami, N.; Chemisana, D.; Rosell, J.; Mallick, T.K. Performance analysis of a dielectric based 3D building integrated concentrating photovoltaic system. *Sol. Energy* **2014**, *103*, 525–540. [\[CrossRef\]](#)
35. Ceylan, I.; Gürel, A.E.; Ergün, A.; Ali IH, G.; Ağbulut, Ü.; Yıldız, G. A detailed analysis of CPV/T solar air heater system with thermal energy storage: A novel winter season application. *J. Build. Eng.* **2021**, *42*, 103097. [\[CrossRef\]](#)
36. Jose, L.S.; Vallerotto, G.; Herrero, R.; Antón, I. Misalignments measurement of CPV optical components through image acquisition. *Opt. Express* **2020**, *28*, 15652–15662. [\[CrossRef\]](#)
37. Felsberger, R.; Buchroithner, A.; Gerl, B.; Wegleiter, H. Conversion and Testing of a Solar Thermal Parabolic Trough Collector for CPV-T Application. *Energies* **2022**, *13*, 6142. [\[CrossRef\]](#)
38. Wen, G. Optical reflection essence of surface-mirror imaging. *Optik* **2022**, *268*, 169822. [\[CrossRef\]](#)
39. Shi, W.; Li, Y.; Chen, R.; Zhang, C.; Liu, Z.; Xie, H.; Liu, F. Research on synchronous measurement technique of temperature and deformation fields using multispectral camera with bilateral telecentric lens. *Theor. Appl. Mech. Lett.* **2022**, *12*, 100345. [\[CrossRef\]](#)
40. Barrios, J.P.L.G.; Cortez, J.R.; Herman, G.M.; Larroder, A.; Jeco, B.M.Y.; Watanabe, K.; Okada, Y. The use of convex lens as primary concentrator for multi-junction solar cells. *Emergent Sci.* **2018**, *2*, 5. [\[CrossRef\]](#)
41. Tien, N.X.; Shin, S. A Novel Concentrator Photovoltaic (CPV) System with the Improvement of Irradiance Uniformity and the Capturing of Diffuse Solar Radiation. *Appl. Sci.* **2016**, *6*, 251. [\[CrossRef\]](#)
42. Winston, R.; Miñano, J.C.; Benítez, P. *Nonimaging Optics*; Elsevier Academic Press: Amsterdam, The Netherlands, 2005.
43. Tiruneh, A.T.; Ndlela, W.N.; Gadaga, T.H.; Debesay, T.; Heikkilä, J. A Four-Wing Compound Parabolic Concentrator (CPC) Design for Heating and Sanitization of Waste Products. *J. Power Energy Eng.* **2017**, *05*, 18–35. [\[CrossRef\]](#)
44. Rosengarten, G.; Stanley, C.; Ferrari, D.; Blakers, A.; Ratcliff, T. The rise of non-imaging optics for rooftop solar collectors. In *Nonimaging Optics: Efficient Design for Illumination and Solar Concentration XIII—Commemorating the 50th Anniversary of Nonimaging Optics*; SPIE: San Diego, CA, USA, 2016.
45. Peharz, G.; Ferrer Rodríguez, J.P.; Siefer, G.; Bett, A.W. Investigations on the temperature dependence of CPV modules equipped with triple-junction solar cells. *Prog. Photovolt. Res. Appl.* **2010**, *19*, 54–60. [\[CrossRef\]](#)
46. Indira, S.S.; Vaithilingam, C.A.; Sivasubramanian, R.; Chong, K.-K.; Saidur, R.; Narasingamurthi, K. Optical performance of a hybrid compound parabolic concentrator and parabolic trough concentrator system for dual concentration. *Sustain. Energy Technol. Assess.* **2021**, *47*, 101538. [\[CrossRef\]](#)
47. Xie, W.; Dai, Y.; Wang, R.; Sumathy, K. Concentrated solar energy applications using Fresnel lenses: A review. *Renew. Sustain. Energy Rev.* **2011**, *15*, 2588–2606. [\[CrossRef\]](#)
48. George, M.; Pandey, A.; Rahim, N.A.; Saidur, R. Recent studies in concentrated photovoltaic system (CPV): A review. In *Proceedings of the 5th IET International Conference on Clean Energy and Technology (CEAT2018)*, Kuala Lumpur, Malaysia, 5–6 September 2018.
49. Kechiche, O.B.H.B.; Hamza, M. Enhancement of a commercial PV module performance under Low Concentrated Photovoltaic (LCPV) conditions: A numerical study. *Renew. Energy Focus* **2022**, *41*, 258–267. [\[CrossRef\]](#)
50. Scarabelot, L.T.; Rambo, C.R.; Rampinelli, G.A. A relative power-based adaptive hybrid model for DC/AC average inverter efficiency of photovoltaics systems. *Renew. Sustain. Energy Rev.* **2018**, *92*, 470–477. [\[CrossRef\]](#)
51. Peharz, G.; Frank, D. Energy payback time of the high-concentration PV system FLATCON®. *Prog. Photovolt. Res. Appl.* **2005**, *13*, 627–634. [\[CrossRef\]](#)

52. Ferrer-Rodríguez, J.P.; Valera, A.; Fernández, E.F.; Almonacid, F.; Pérez-Higueras, P. Ray Tracing Comparison between Triple-Junction and Four-Junction Solar Cells in PMMA Fresnel-Based High-CPV Units. *Energies* **2018**, *11*, 2455. [\[CrossRef\]](#)
53. Roychoudhuri, C. *Fundamentals of Photonics*; SPIE: Bellingham, WA, USA, 2008; Volume TT79, pp. 73–116.
54. Xie, P.; Lin, H.; Liu, Y.; Li, B. Total internal reflection-based planar waveguide solar concentrator with symmetric air prisms as couplers. *Opt. Express* **2014**, *22*, A1389–A1398. [\[CrossRef\]](#)
55. Liang, S.; Zheng, H.; Liu, S.; Ma, X. Optical design and validation of a solar concentrating photovoltaic-thermal (CPV-T) module for building louvers. *Energy* **2022**, *239*, 122256. [\[CrossRef\]](#)
56. Lovegrove, K.; Stein, W. *Concentrating Solar Power Technology Principles, Developments, and Applications*, 2nd ed.; Woodhead Publishing Limited: Cambridge, UK, 2020.
57. Blanco, M.J.; Santigosa, L.R. *Improved Design for Linear Fresnel Reflector Systems*; Woodhead Publishing Series in Energy: Cambridge, UK, 2017.
58. Zagolla, V.; Dominé, D.; Tremblay, E.; Moser, C. Self-tracking solar concentrator with an acceptance angle of 32°. *Opt. Express* **2014**, *22*, 1880–1894. [\[CrossRef\]](#)
59. Alzahrani, M.; Ahmed, A.; Shanks, K.; Sundaram, S.; Mallick, T. Optical component analysis for ultrahigh concentrated photovoltaic system (UHCPV). *Sol. Energy* **2021**, *227*, 321–333. [\[CrossRef\]](#)
60. Singh, H.; Sabry, M.; Redpath, D. Experimental investigations into low concentrating line axis solar concentrators for CPV applications. *Sol. Energy* **2016**, *136*, 421–427. [\[CrossRef\]](#)
61. Vu, H.; Vu, N.H.; Shin, S. Static Concentrator Photovoltaics Module for Electric Vehicle Applications Based on Compound Parabolic Concentrator. *Energies* **2022**, *15*, 6951. [\[CrossRef\]](#)
62. Linderman, R.J.; Judkins, Z.S.; Shoecraft, M.; Dawson, M.J. Thermal Performance of the SunPower Alpha-2 PV Concentrator. *IEEE J. Photovolt.* **2012**, *2*, 196–201. [\[CrossRef\]](#)
63. Chaudhary, G.Q.; Kousar, R.; Ali, M.; Amar, M.; Amber, K.P.; Lodhi, S.K.; Din, M.R.; Ditta, A. Small-Sized Parabolic Trough Collector System for Solar Dehumidification Application: Design. *Int. J. Photoenergy* **2018**, *2018*, 5759034. [\[CrossRef\]](#)
64. Vu, D.T.; Vu, N.H.; Shin, S.; Pham, T.T. Cylindrical Fresnel lens: An innovative path toward a tracking-less concentrating photovoltaics system. *Sol. Energy* **2022**, *234*, 251–261. [\[CrossRef\]](#)
65. Wang, G.; Wang, F.; Shen, F.; Jiang, T.; Chen, Z.; Hu, P. Experimental and optical performances of a solar CPV device using a linear Fresnel reflector concentrator. *Renew. Energy* **2020**, *146*, 2351–2361. [\[CrossRef\]](#)
66. Himer, S.E.; Ayane, S.E.; Yahyaoui, S.E.; Salvestrini, J.P.; Ahaitouf, A. Photovoltaic Concentration: Research and Development. *Energies* **2020**, *13*, 5721. [\[CrossRef\]](#)
67. Felsberger, R.; Buchroithner, A.; Gerl, B.; Schweighofer, B.; Preßmair, R.; Mitter, T.; Wegleiter, H. Optical performance and alignment characterization of a parabolic trough collector using a multi-junction CPV solar cell. *Sol. Energy* **2022**, *239*, 40–49. [\[CrossRef\]](#)
68. Renno, C.; Perone, A. Experimental modeling of the optical and energy performances of a point-focus CPV system applied to a residential user. *Energy* **2021**, *215*, 119156. [\[CrossRef\]](#)
69. Iqbal, W.; Ullah, I.; Shin, S. Nonimaging High Concentrating Photovoltaic System Using Trough. *Energies* **2023**, *16*, 1336. [\[CrossRef\]](#)
70. Renno, C.; Perone, A.; Pirone, V. Comparison of the Spherical Optics and Fresnel Lens Performance in a Point-Focus CPV System applied to a residential user. *Int. Energy J.* **2022**, *22*, 1–12.
71. Teng, T.C.; Kuo, C.H.; Li, Y.J. Planar solar concentrator composed of stacked waveguides with arc-segment structures and movable receiving assemblies. *Opt. Express* **2020**, *28*, 34362–34377. [\[CrossRef\]](#)
72. Miñano, J.C.; Benítez, P.; Zamora, P.; Buljan, M.; Moledano, R.; Santamaría, A.J.O.E. Free-form optics for Fresnel-lens-based photovoltaic concentrators. *Opt. Express* **2013**, *21*, A494–A502. [\[CrossRef\]](#)
73. Ferrer-Rodríguez, J.P.; Fernández, E.F.; Almonacid, F.; Pérez-Higueras, P. Optical design of a 4-off-axis-unit Cassegrain ultra-high concentrator photovoltaics module with a central receiver. *Opt. Lett.* **2016**, *41*, 1985–1988. [\[CrossRef\]](#)
74. Shanks, K.; Ferrer-Rodríguez, J.P.; Fernández, E.F.; Almonacid, F.; Pérez-Higueras, P.; Senthilarasu, S.; Mallick, T. A > 3000 suns high concentrator photovoltaic design based on multiple Fresnel lens primaries focusing to one central solar cell. *Sol. Energy* **2018**, *169*, 457–467. [\[CrossRef\]](#)
75. Ferrer-Rodríguez, J.P.; Saura, J.M.; Fernández, E.F.; Almonacid, F.; Talavera, D.L.; Pérez-Higueras, P. Exploring ultra-high concentrator photovoltaic Cassegrain-Koehler-based designs up to 6000×. *Opt. Express* **2020**, *28*, 6609–6617. [\[CrossRef\]](#)
76. Alzahrani, M.; Shanks, K.; Mallick, T.K. Advances and limitations of increasing solar irradiance for concentrating photovoltaics thermal system. *Renew. Sustain. Energy Rev.* **2021**, *138*, 110517. [\[CrossRef\]](#)
77. Rahmanian, S.; Moein-Jahromi, M.; Rahmanian-Koushkaki, H.; Sopian, K. Performance investigation of inclined CPV system with composites of PCM, metal foam and nanoparticles. *Sol. Energy* **2021**, *230*, 883–901. [\[CrossRef\]](#)
78. Xiao, M.; Tang, L.; Zhang, X.; Lun, I.Y.F.; Yuan, Y. A Review on Recent Development of Cooling Technologies for Concentrated Photovoltaics (CPV) Systems. *Energies* **2018**, *11*, 3416. [\[CrossRef\]](#)
79. Zhou, Z.; Wang, Z.; Bermel, P. Radiative cooling for low-bandgap photovoltaics under concentrated sunlight. *Opt. Express* **2019**, *27*, A404–A418. [\[CrossRef\]](#)
80. Alzahrani, M.; Roy, A.; Shanks, K.; Sundaram, S.; Mallick, T.K. Graphene as a pre-illumination cooling approach for a concentrator photovoltaic (CPV) system. *Sol. Energy Mater. Sol. Cells* **2021**, *222*, 110922. [\[CrossRef\]](#)

81. Elminshawy, N.; Elminshawy, A.; Osama, A.; Bassyouni, M.; Arıcı, M. Experimental performance analysis of enhanced concentrated photovoltaic utilizing various mass flow rates of Al₂O₃-nanofluid: Energy, exergy, and exergoeconomic study. *Sustain. Energy Technol. Assess.* **2022**, *53*, 102723. [CrossRef]
82. Elminshawy, A.; Morad, K.; Elminshawy, N.A.S.; Elhenawy, Y. Performance enhancement of concentrator photovoltaic systems using nanofluids. *Int. J. Energy Res.* **2021**, *45*, 2959–2979. [CrossRef]
83. Kalogirou, S.A. Chapter 4—Performance of Solar Collectors. In *Solar Energy Engineering Processes and Systems*, 2nd ed.; Academic Press: Cambridge, MA, USA, 2014; pp. 221–256.
84. Martinez, M.; de la Rubia, O.; Rubio, F.; Banda, P. 1.36—Concentration Photovoltaics. In *Comprehensive Renewable Energy*, 2nd ed.; Elsevier: Amsterdam, The Netherlands, 2022; pp. 755–775.
85. Zheng, H. Chapter 2—Solar Energy Utilization and Its Collection Devices. In *Solar Energy Desalination Technology*; Elsevier: Amsterdam, The Netherlands, 2017; pp. 47–171.
86. Aqachmar, Z.; Campana, P.E.; Bouhal, T.; Qarnia, H.E.; Outzourhit, A.; Ibnouelghazi, E.A.; Mouak, S.; Aqachmar, A. Electrification of Africa through CPV installations in small-scale industrial applications: Energetic, economic, and environmental analysis. *Renew. Energy* **2022**, *197*, 723–746. [CrossRef]
87. Ahaitouf, A.; El-Yahyaoui, S.; Elhimer, S.; El-Ayane, S.; Salvestrini, J.-P.; Ougazzaden, A. Simulation and experimental validation in outdoor conditions of a CPV system based on both pyramid and cone secondary optical elements. *Energy Convers. Manag. X* **2022**, *16*, 100278. [CrossRef]
88. Liang, S.; Zheng, H.; Zhao, Z.; Ma, X.; Ng, K.C. Investigation on an underwater solar concentrating photovoltaic-membrane distillation (CPV-MD) integrated system. *Desalination* **2023**, *546*, 116193. [CrossRef]
89. NREL. Solar Spectra. Available online: <https://www.nrel.gov/grid/solar-resource/spectra.html> (accessed on 2 September 2022).
90. Sabry, M.; Lashin, A.; Al Turkestani, M. Experimental and simulation investigations of CPV/TEG hybrid system. *J. King Saud Univ.-Sci.* **2021**, *33*, 101321. [CrossRef]
91. Karimi, F.; Xu, H.; Wang, Z.; Chen, J.; Yang, M. Experimental study of a concentrated PV/T system using linear Fresnel lens. *Energy* **2017**, *123*, 402–412. [CrossRef]
92. Ferrer-Rodríguez, J.P.; Baig, H.; Fernández, E.F.; Almonacid, F.; Mallick, T.; Pérez-Higueras, P. Optical modeling of four Fresnel-based high-CPV units. *Sol. Energy* **2017**, *155*, 805–815. [CrossRef]
93. Burhan, M.; Shahzad, M.W.; Ng, K.C. Long-term performance potential of concentrated photovoltaic (CPV) systems. *Energy Convers. Manag.* **2017**, *148*, 90–99. [CrossRef]
94. Araki, K.; Yano, T.; Kuroda, Y. 30 kW Concentrator Photovoltaic System Using Dome-shaped Fresnel Lenses. *Opt. Express* **2010**, *18*, A53–A63. [CrossRef]
95. Himer, S.E.; Ahaitouf, A. Improvement of Optical Performances Using the Hybrid CPV. *J. Daylighting* **2020**, *7*, 238–245. [CrossRef]
96. Zamora, P.; Benítez, P.; Mohedano, R.; Cvetkovic, A.; Vilaplana, J.; Li, Y.; Hernandez, M.; Chaves, J.; Miñano, J.C. Experimental characterization of Fresnel-Köhler concentrators. *J. Photon. Energy* **2012**, *2*, 021806. [CrossRef]
97. Araki, K.; Zamora, P.; Nagai, H.; Benitez, P.; Hobo, K.; Miñano, J.C.; Futo, M.; Sala, G.; Tamura, K.; Kumagai, I. Design and development of 35% efficient and 1000X CPV module with sufficient optical alignment tolerance. In Proceedings of the 2012 38th IEEE Photovoltaic Specialists Conference, Austin, TX, USA, 3–8 June 2012.
98. Mendes-Lopes, J.; Benítez, P.; Zamora, P.; Miñano, J.C.J.O.E. 9-fold Fresnel-Köhler concentrator with Fresnel lens of variable focal point. *Opt. Express* **2014**, *22*, A1153–A1163. [CrossRef]
99. Zou, Y.-H.; Yang, T.-S. Optical performance analysis of a HCPV solar concentrator yielding highly uniform cell irradiance. *Sol. Energy* **2014**, *107*, 1–11. [CrossRef]
100. Fischer, S.; Ivaturi, A.; Frohlich, B.; Rudiger, M.; Richter, A.; Kramer, K.W.; Richards, B.S.; Goldschmidt, J.C. Upconverter Silicon Solar Cell Devices for Efficient Utilization of Sub-Band-Gap Photons Under Concentrated Solar Radiation. *IEEE J. Photovolt.* **2014**, *4*, 183–189. [CrossRef]
101. Victoria, M.; Askins, S.; Herrero, R.; Antón, I.; Sala, G. Assessment of the optical efficiency of a primary lens to be used in a CPV system. *Sol. Energy* **2016**, *134*, 406–415. [CrossRef]
102. Huang, Q.; Liao, T.; Xu, L. Design and preliminary experiments of truncated ball lens as secondary optical element for CPV system. *Sol. Energy* **2018**, *169*, 19–23. [CrossRef]
103. Martinez, J.F.; Steiner, M.; Wiesenfarth, M.; Glunz, S.W.; Dimroth, F. Thermal Analysis of Passively Cooled Hybrid CPV Module Using Si Cell as Heat Distributor. *IEEE J. Photovolt.* **2019**, *9*, 160–166. [CrossRef]
104. Stanek, B.; Grzywnowicz, K.; Bartela, Ł.; Węcel, D.; Uchman, W. A system analysis of hybrid solar PTC-CPV absorber operation. *Renew. Energy* **2021**, *174*, 635–653. [CrossRef]
105. Wang, G.; Zhang, Z.; Chen, Z. Design and performance evaluation of a novel CPV-T system using nano-fluid spectrum filter and with high solar concentrating uniformity. *Energy* **2023**, *267*, 126616. [CrossRef]
106. Mohsenzadeh, M.; Shafii, M.; Mosleh, H.J. A novel concentrating photovoltaic/thermal solar system combined with thermoelectric module in an integrated design. *Renew. Energy* **2017**, *113*, 822–834. [CrossRef]
107. Ullah, I. Optical modeling of two-stage concentrator photovoltaic system using parabolic trough. *J. Photon- Energy* **2019**, *9*, 043102. [CrossRef]
108. Cooper, T.; Ambrosetti, G.; Pedretti, A.; Steinfeld, A. Surpassing the 2D Limit: A 600× High-concentration PV Collector Based on a Parabolic trough with Tracking Secondary Optics. *Energy Procedia* **2014**, *57*, 285–290. [CrossRef]

109. Norman, R.; Leveille, E.; Caillou, N.; Blais, J.; Rosa, S.; Aimez, V.; Frechette, L.G. Molding arrays of tertiary optical elements for microcell receivers. In *AIP Conference Proceedings*; AIP Publishing LLC: Melville, NY, USA, 2022; p. 2550. [\[CrossRef\]](#)
110. Cooper, T.; Ambrosetti, G.; Pedretti, A.; Steinfeld, A. Theory and design of line-to-point focus solar concentrators with tracking secondary optics. *Appl. Opt.* **2013**, *52*, 8586–8616. [\[CrossRef\]](#)
111. Schmitz, M.; Cooper, T.; Ambrosetti, G.; Steinfeld, A. Two-stage solar concentrators based on parabolic troughs: Asymmetric versus symmetric designs. *Appl. Opt.* **2015**, *54*, 9709–9721. [\[CrossRef\]](#) [\[PubMed\]](#)
112. Cooper, T.; Ambrosetti, G.; Malnati, F.; Pedretti, A.; Steinfeld, A. Experimental demonstration of high-concentration photovoltaics on a parabolic trough using tracking secondary optics. *Prog. Photovolt. Res. Appl.* **2016**, *24*, 1410–1426. [\[CrossRef\]](#)
113. Riahi, A.; Ali, A.B.H.; Fadhel, A.; Guizani, A.; Balghouthi, M. Performance investigation of a concentrating photovoltaic thermal hybrid solar system combined with thermoelectric generators. *Energy Convers. Manag.* **2020**, *205*, 112377. [\[CrossRef\]](#)
114. Ullah, I. Fiber-based daylighting system using trough collector for uniform illumination. *Sol. Energy* **2019**, *196*, 484–493. [\[CrossRef\]](#)
115. Felsberger, R.; Buchroithner, A.; Gerl, B.; Schweighofer, B.; Wegleiter, H. Design and testing of concentrated photovoltaic arrays for retrofitting of solar thermal parabolic trough collectors. *Appl. Energy* **2021**, *300*, 117427. [\[CrossRef\]](#)
116. Orosz, M.; Dickes, R. 16—Solar thermal powered Organic Rankine Cycles. In *Organic Rankine Cycle (ORC) Power Systems Technologies and Applications*; Woodhead Publishing: Delhi, India, 2017; pp. 569–612.
117. Kalogirou, S. Nontracking solar collection technologies for solar heating and cooling systems. In *Advances in Solar Heating and Cooling*; Woodhead Publishing Series in Energy: Delhi, India, 2016; pp. 63–80. [\[CrossRef\]](#)
118. Parthiban, A.; Mallick, T.; Reddy, K. Integrated optical-thermal-electrical modeling of compound parabolic concentrator based photovoltaic-thermal system. *Energy Convers. Manag.* **2022**, *251*, 115009. [\[CrossRef\]](#)
119. Lokeswaran, S.; Mallick, T.K.; Reddy, K. Design and analysis of dense array CPV receiver for square parabolic dish system with CPC array as secondary concentrator. *Sol. Energy* **2020**, *199*, 782–795. [\[CrossRef\]](#)
120. Baig, H.; Sellami, N.; Bahaidarah, H.; Mallick, T. Optical Analysis of a CPC Based CPV/T System for Application in the Kingdom of Saudi Arabia. In *Proceedings of the 28th European Photovoltaic Solar Energy Conference and Exhibition*, Paris, France, 30 September–4 October 2013; pp. 653–657. [\[CrossRef\]](#)
121. Karp, J.H.; Tremblay, E.J.; Ford, J.E. Planar micro-optic solar concentrator. *Opt. Express* **2010**, *18*, 1122–1133. [\[CrossRef\]](#) [\[PubMed\]](#)
122. Teng, T.-C.; Lai, W.-C. Planar solar concentrator featuring alignment-free total-internal-reflection collectors and an innovative compound tracker. *Opt. Express* **2014**, *22*, A1818–A1834. [\[CrossRef\]](#)
123. Moore, D.; Schmidt, G.; Unger, B. Concentrated photovoltaics stepped planar light guide. In *Proceedings of the SPIE 7652, International Optical Design Conference 2010*, Jackson Hole, WY, USA, 13–17 June 2010.
124. Ramachandran, A.M.; Sangeetha, M.S.; Thampi, A.S.; Singh, M.; Asok, A. A comprehensive review on optics and optical materials for planar waveguide-based compact concentrated solar photovoltaics. *Results Eng.* **2022**, *16*, 100665. [\[CrossRef\]](#)
125. Dhakal, R.; Lee, J.; Kim, J. Bio-inspired thin and flat solar concentrator for efficient, wide acceptance angle light collection. *Appl. Opt.* **2014**, *53*, 306–315. [\[CrossRef\]](#) [\[PubMed\]](#)
126. Nakatani, M.; Yamada, N. Optical Analysis of Secondary Optical Element for Microtracking CPV System with Core-shell Spherical Lens. In *Proceedings of the 2019 IEEE 46th Photovoltaic Specialists Conference (PVSC)*, Chicago, IL, USA, 16–21 June 2019; pp. 0264–0267. [\[CrossRef\]](#)
127. Terao, A.; Mulligan, W.; Daroczi, S.; Pujol, O.; Verlinden, P.; Swanson, R.; Minano, J.; Benitz, P.; Alvarez, J.L. A mirror-less design for micro-concentrator modules. In *Proceedings of the Conference Record of the Twenty-Eighth IEEE Photovoltaic Specialists Conference—2000*, Anchorage, AK, USA, 15–22 September 2000.
128. Kechiche, O.B.H.B.; Sammouda, H. Concentrator Photovoltaic System (CPV): Maximum Power Point Techniques (MPPT) Design and Performance. In *Solar Radiation—Measurement, Modeling and Forecasting Techniques for Photovoltaic Solar Energy Applications*; IntechOpen: London, UK, 2022.
129. Cai, Z.; Zhao, C.; Zhao, Z.; Yao, X.; Zhang, H.; Zhang, Z. Highly Efficient Solar Laser Pumping Using a Solar Concentrator Combining a Fresnel Lens and Modified Parabolic Mirror. *Energies* **2022**, *15*, 1792. [\[CrossRef\]](#)
130. Cisneros-Cárdenas, N.A.; Cabanillas-López, R.; Pérez-Enciso, R.; Martínez-Rodríguez, G.; García-Gutiérrez, R.; Pérez-Rábago, C.; Calleja-Valdez, R.; Riveros-Rosas, D. Study of the Radiation Flux Distribution in a Parabolic Dish Concentrator. *Energies* **2021**, *14*, 7053. [\[CrossRef\]](#)
131. Chou, T.-L.; Shih, Z.-H.; Hong, H.-F.; Han, C.-N.; Chiang, K.-N. Thermal Performance Assessment and Validation of High-Concentration Photovoltaic Solar Cell Module. *IEEE Trans. Compon. Packag. Manuf. Technol.* **2012**, *2*, 578–586. [\[CrossRef\]](#)
132. Zhuang, Z.; Yu, F. Compact Flyeye concentrator with improved irradiance uniformity on solar cell. *Opt. Eng.* **2013**, *52*, 087108. [\[CrossRef\]](#)
133. Coughenour, B.M.; Stalcup, T.; Wheelwright, B.; Geary, A.; Hammer, K.; Angel, R. Dish-based high concentration PV system with Köhler optics. *Opt. Express* **2014**, *22*, A211–A224. [\[CrossRef\]](#)
134. Cappelletti, A.; Catelani, M.; Ciani, L.; Kazimierczuk, M.K.; Reatti, A. Practical Issues and Characterization of a Photovoltaic/Thermal Linear Focus $20\times$ Solar Concentrator. *IEEE Trans. Instrum. Meas.* **2016**, *65*, 2464–2475. [\[CrossRef\]](#)
135. Jost, N.; Domínguez, C.; Vallerotto, G.; Gu, T.; Hu, J.; Antón, I. Novel optical approach for concentrating light in micro-CPV. In *Proceedings of the 2019 IEEE 46th Photovoltaic Specialists Conference (PVSC)*, Chicago, IL, USA, 16–21 June 2019.

136. Araki, K.; Lee, K.-H.; Hayashi, N.; Ichihashi, K.; Kanayama, S.; Inohara, T.; Morita, Y.; Takase, M.; Yamaguchi, M. Design of the Micro-Köhler Concentrator Optics for CPV Application. In Proceedings of the 2019 IEEE 46th Photovoltaic Specialists Conference (PVSC), Chicago, IL, USA, 16–21 June 2019.
137. Zhang, F.; Wenham, S.; Green, M. Large area, concentrator buried contact solar cells. *IEEE Trans. Electron Devices* **1995**, *42*, 144–149. [CrossRef]
138. Jared, B.H.; Saavedra, M.P.; Anderson, B.J.; Goeke, R.S.; Sweatt, W.C.; Nielson, G.N.; Okandan, M.; Elisberg, B.; Snively, D.; Duncan, J.; et al. Micro-concentrators for a microsystems-enabled photovoltaic system. *Opt. Express* **2014**, *22*, A521–A527. [CrossRef]
139. Li, D. DSpace@MIT. 2020. Available online: <https://dspace.mit.edu/handle/1721.1/123563?show=full> (accessed on 13 March 2023).
140. Reuna, J.; Hietalahti, A.; Aho, A.; Isoaho, R.; Aho, T.; Vuorinen, M.; Tukiainen, A.; Anttola, E.; Guina, M. Optical Performance Assessment of Nanostructured Alumina Multilayer Antireflective Coatings Used in III–V Multijunction Solar Cells. *ACS Appl. Energy Mater.* **2022**, *5*, 5804–5810. [CrossRef] [PubMed]
141. Schygulla, P.; Müller, R.; Lackner, D.; Höhn, O.; Hauser, H.; Bläsi, B.; Predan, F.; Benick, J.; Hermle, M.; Glunz, S.W.; et al. Two-terminal III–V//Si triple-junction solar cell with power conversion efficiency of 35.9% at AM1.5g. *Prog. Photovolt. Res. Appl.* **2021**, *30*, 869–879. [CrossRef]
142. Albert, P.; Jaouad, A.; Hamon, G.; Volatier, M.; Valdivia, C.E.; Deshayes, Y.; Hinzer, K.; Béchou, L.; Aimez, V.; Darnon, M. Miniaturization of InGaP/InGaAs/Ge solar cells for micro-concentrator photovoltaics. *Prog. Photovolt. Res. Appl.* **2021**, *29*, 990–999. [CrossRef]
143. Renno, C. Characterization of spherical optics performance compared to other types of optical systems in a point-focus CPV system. *Therm. Sci. Eng. Prog.* **2022**, *29*, 101201. [CrossRef]
144. SHARP. 2022. Available online: <https://global.sharp/corporate/news/220606-a.html> (accessed on 17 May 2023).
145. Timpano, M.D.; Cooper, T.A. Nonimaging Behavior of Circular Trough Concentrators with Tubular Receivers. *J. Sol. Energy Eng.* **2023**, *146*, 1–32. [CrossRef]
146. Korres, D.N.; Tzivanidis, C. A flat plate collector with a multi-cavity receiver as an innovative alternative in contrast to the classical design: A comparative study with experimental validation. *Therm. Sci. Eng. Prog.* **2023**, *42*, 101874. [CrossRef]
147. Stanek, B.; Ochmann, J.; Węcel, D.; Bartela, Ł. Study of Twisted Tape Inserts Segmental Application in Low-Concentrated Solar Parabolic Trough Collectors. *Energies* **2023**, *16*, 3716. [CrossRef]
148. Santos, D.; Azgin, A.; Castro, J.; Kizildag, D.; Rigola, J.; Tunçel, B.; Turan, R.; Preßmair, R.; Felsberger, R.; Buchroithner, A. Thermal and fluid dynamic optimization of a CPV-T receiver for solar co-generation applications: Numerical modelling and experimental validation. *Renew. Energy* **2023**, *211*, 87–99. [CrossRef]
149. Beltagy, H. A secondary reflector geometry optimization of a Fresnel type solar concentrator. *Energy Convers. Manag.* **2023**, *284*, 116974. [CrossRef]
150. Hosouli, S.; Gomes, J.; Jahangir, M.T.; Pius, G. Performance Evaluation of Novel Concentrating Photovoltaic Thermal Solar Collector under Quasi-Dynamic Conditions. *Solar* **2023**, *3*, 195–212. [CrossRef]

Disclaimer/Publisher’s Note: The statements, opinions and data contained in all publications are solely those of the individual author(s) and contributor(s) and not of MDPI and/or the editor(s). MDPI and/or the editor(s) disclaim responsibility for any injury to people or property resulting from any ideas, methods, instructions or products referred to in the content.